Title

Impact of increased APP gene dose in Down syndrome and the Dp16 mouse model

Journal

Alzheimer's & Dementia, 18(6)

ISSN

1552-5260

Authors

Sawa, Mariko
Overk, Cassia
Becker, Ann
et al.

Publication Date

2022-06-01

DOI

10.1002/alz.12463

Peer reviewed

Published in final edited form as:

Alzheimers Dement. 2022 June ; 18(6): 1203–1234. doi:10.1002/alz.12463.

Impact of Increased APP Gene Dose in Down Syndrome and the Dp16 Mouse Model

Mariko Sawa[1], **Cassia Overk**[1], **Ann Becker**[1], **Dominique Derse**[1], **Ricardo Albay**[1], **Kim Weldy**[1], **Ahmad Salehi**[2], **Thomas G. Beach**[3], **Eric Doran**[4], **Elizabeth Head**[5], **Y. Eugene Yu**[6], **William C Mobley**[1,*]

[1]Department of Neurosciences, University of California San Diego, La Jolla, CA, 92093-0624

[2]Department of Psychiatry and Behavioral Sciences, Stanford University, Stanford, CA, 94305

[3]Brain and Body Donation Program, Banner Sun Health Research Institute, Sun City, AZ 85351

[4]Department of Pediatrics, University of California, Irvine, CA, 92697

[5]Department of Pathology & Laboratory Medicine, University of California, Irvine, CA, 92697

[6]The Children's Guild Foundation Down Syndrome Research Program, Genetics and Genomics Program, Roswell Park Comprehensive Cancer Center, Buffalo, NY 14263

Abstract

INTRODUCTION: People with Down syndrome (DS) are predisposed to Alzheimer's disease (AD). The amyloid hypothesis informs studies of AD. In AD-DS, but not sporadic AD, increased *APP* copy number is necessary, defining the *APP* gene dose hypothesis. Which *APP* products contribute needs to be determined.

METHODS: Brain levels of fl-hAPP, C-terminal fragments (hCTFs), and Aβ peptides were measured in DS, AD-DS, non-demented controls (ND) and sporadic AD cases. The *APP* gene-dose hypothesis was evaluated in the Dp16 model.

RESULTS: DS and AD-DS differed from ND and AD for all *APP* products. In AD-DS, Aβ42 and Aβ40 levels exceeded AD. *APP* products were increased in the Dp16 model; increased *APP* gene dose was necessary for loss of vulnerable neurons, tau pathology, and activation of astrocytes and microglial.

DISCUSSION: Increases in *APP* products other than Aβ distinguished AD-DS from AD. Deciphering AD-DS pathogenesis necessitates deciphering which *APP* products contribute and how.

*Correspondence to: William Mobley M.D., Department of Neurosciences, UCSD School of Medicine, 9500 Gilman Drive, GPL 355, La Jolla, CA 92093-0624; wmobley@ucsd.edu.

Author contributions

MS, CO, AB, and WM were involved in the study conception. MS, CO, AB, DD, RA, and WM were involved in data processing and interpretation. MS, CO, and WM wrote the manuscript. All authors contributed to revising the manuscript and were involved in the acquisition of data, procurement of samples, acquisition of molecular data, or provision of comparison data sets. All authors have approved the final manuscript.

Keywords

Alzheimer's disease; trisomy 21; Dp16; neurodegeneration; sex differences

Narrative

The ongoing epidemic of Alzheimer's disease (AD) [1] motivates studies to understand underlying pathological mechanisms and discover treatments to prevent or ameliorate dementia. Regarding these objectives, it is noteworthy that the most common genetic cause for AD is Down syndrome (DS) [1]. By deciphering the genetic and mechanistic basis for AD in DS (AD-DS) it may be possible to accelerate progress toward treatments for those with DS as well as for those with sporadic and other genetic causes of AD. An important step is discovering the responsible gene(s) and mechanisms. Studies in DS point compellingly to a third copy of the gene for APP as necessary for AD, but how increased APP dose confers increased risk for AD is unknown. The existing literature suggested that increased *APP* dose would be correlated with increased levels of APP products in the DS and AD-DS brain. However, few quantitative studies had been undertaken, especially a comparison of the levels of APP products in DS and AD-DS versus AD. Herein, we addressed the impact of increased *APP* dose by examining the full-length protein (fl-hAPP) as well as its C-terminal fragments (hCTFs) and Aβ peptides in the brains of those with DS and AD-DS, comparing their levels to those in non-demented (ND) controls and in patients with AD. We reasoned that increases in APP products, including possible deviations from dose-linked proportional increases, would nominate *APP* products for a role in AD-DS. The differences we discovered differentiated DS and AD-DS from both ND controls and AD. The resulting updated hypothesis points to the possibility that several APP products may contribute to pathogenesis in DS and AD-DS brains and encourages studies for deciphering the impact of *APP* dose that go beyond the amyloid hypothesis.

DS, the most common survivable aneuploidy, occurs in ~1 in 800 births [2]; there are more than 250,000 people in the US with DS [3, 4]. In 95% of cases, DS is caused by trisomy for an entire copy of chromosome 21 [5–8]. The syndrome features characteristic changes in many organ systems and tissues. Nearly universal are difficulties with cognitive development in children and emergence of dementia in adults [9–11]. The impact of brain disorders in DS motivates studies to explicate the genetic and cellular bases. Manifestations in DS are due, directly or indirectly, to the triplication of a gene(s), an extra copy of regulatory sequences, or other chromosomal material on human chromosome 21 (HSA21) [5, 12]. Advances in genetics and cellular biology in the past two decades enabled studies to define the genes underlying the changes (i.e., phenotypes) induced by trisomy for HSA21. The chromosome contains 235 protein-encoding genes, 423 non-protein-coding genes, and 188 pseudo-genes (reviewed in [5]). Cognitive deficits may be linked to an increased dose of several HSA21 genes [5, 13, 14], as well as HSA21 gene dose-induced changes in the expression of genes on other chromosomes [15–17]. Indeed, a recent comprehensive study of gene expression in the DS brain examining tissue at ages from 14 post-conception weeks to age 42 years demonstrated genome-wide changes in expression pointing to the involvement of distinct biological pathways and all brain cell types [16].

Of the many medical comorbidities present in adults with DS [1, 18], the most significant for those beyond age 40 years is dementia. Similarities to Alzheimer's disease (AD) in clinical presentation and the striking concordance of neuropathological features enable a diagnosis of AD in DS – i.e., AD-DS [10, 11]. As for AD, the neuropathology of AD-DS includes the presence of neuritic amyloid plaques containing the Aβ peptide product of the human amyloid precursor protein (hAPP) and neurofibrillary tangles containing phosphorylated isoforms of tau [19–21]. Also, in the context of increasing neurofibrillary pathology, microglia show dystrophic processes in the fifth decade [22]. Less well appreciated is the enlargement of early endosomes, a change present in early AD and present in the DS brain as early as the fetal period [19, 23, 24]. While the pathological diagnosis of AD-DS can be made in essentially all those with DS by the age of 40 years [25], the average age of clinical diagnosis of dementia is ~56 years, with more than 80% affected by age 69 [5, 11, 26].

Despite the complex genetic environment created by an entire extra chromosome, it is remarkable that an extra copy of a single gene, Amyloid Precursor Protein (h*APP*) located on HSA21, is essential for AD-DS. h*APP* encodes a highly conserved Type 1 integral membrane protein (fl-hAPP) that is highly expressed in CNS neurons. Compelling evidence for an essential role for increased h*APP* gene dose for AD-DS is case reports in which a person partially trisomic for HSA21, and carrying only two copies of the h*APP* gene, demonstrated neither the pathology of AD nor became demented even in old age [27, 28]. h*APP* multiplications and missense mutations have also been linked to familial and sporadic forms of AD [29]. Thus, increased h*APP* gene dose is also sufficient for a form of familial AD (FAD) [30, 31].

It is essential to decipher how increased h*APP* gene dose induces AD pathogenesis. Given that increased APP dose is not present in sporadic AD, one must question whether the amyloid hypothesis for AD suffices to explain pathogenesis in those with DS. Toward understanding AD-DS it is essential to demonstrate that the extra copy of *APP* results in increased levels of its products, an expectation not well established. Indeed, relatively few studies quantitatively document levels of fl-hAPP and its products in the DS brain, and only one directly compared the levels to those in AD. An early study linked gene-dose to increases in fl-hAPP and Aβ in DS in the brains of DS and AD cases, but the number of DS samples whose age puts them at increased risk for AD-DS was very small [32]. Relative to controls, later reports showed that increased h*APP* gene dose in DS is reflected in increases in the levels of gene expression at the levels of *APP* mRNA [33, 34], fl-hAPP [32, 35–38], and its C-terminal fragments (CTFs) [34, 37, 39–41]. Aβ peptides in the brain and plasma are also increased in DS [32, 36, 37, 42–48] and CSF Aβ42 levels demonstrate decreases coincident with cognitive decline, as in AD [47].

To explore how increased *APP* gene dose is linked to AD-DS, we tested the hypothesis that increased dose is registered in increases in fl-hAPP and its products in those whose age puts them at risk for this diagnosis. We reasoned that *APP* products potentially relevant to pathogenesis would be present in the DS and AD-DS brain at levels increased relative to ND controls and possibly to AD. In pathologically and clinically characterized cases of DS and AD-DS we quantitatively examined brain levels of *APP* products. Our studies employed

detergent soluble lysates of the frozen prefrontal cortex in which the levels of fl-hAPP, hCTFs, Aβ42, Aβ40, and Aβ38 were measured.

We discovered that DS and AD-DS samples differed significantly from ND controls and AD in all measures. Increased *APP* dose resulted in increases in fl-hAPP proportional to gene dose. Greater than proportional increases were seen in Aβ42 and Aβ40, with levels that exceeded by several-fold those in AD. Increased hCTFS were present in males and females in DS and AD-DS; only in females did the levels exceed the increases in fl-hAPP. These findings support the hypothesis and point to the possibility that several APP products could contribute to pathogenesis. They also suggest *APP* dose-mediated changes in processing and clearance of *APP* products as a possible contributor.

Limitations inherent in the use of human tissue include that the values measured provide but a 'snapshot' of APP products, one that is possibly impacted by premortem status. Moreover, our measures were undertaken only in older adults, obviating the ability to define and quantitate possible age-related changes. Equally limiting, postmortem samples do not support the ability to discriminate between cause and effect. However informative are such studies, they do not readily admit of the ability to define which *APP* product(s) is responsible for neurodegeneration, how it acts, and when it does so. To ask such questions we determined if the changes in DS and AD-DS were recapitulated in a mouse model of DS. In the Dp16 model, increases for fl-mAPP, mCTFs, Aβ 40, and 42 were proportional to *APP* dose. Age-related increases in Aβ40 and 42 were detected in both Dp16 and 2N mice. Significantly, we found *APP* dose-dependent degeneration of vulnerable neurons. Moreover, tau pathology and activation of astrocytes and microglial also responded to increased *APP* dose. Finally, enlargement of early endosomes was also linked to increased *APP*. Studies in the model further inform the hypothesis, and importantly, converge with human data to demonstrate the necessity of increased *APP* dose for neurodegeneration in DS.

Taken together with other studies our findings point to increased *APP* dose leading to essentially life-long increases in *APP* products in both humans with DS and the Dp16 model. In so doing they point to the possibility that the mechanisms responsible for AD-DS are active decades before disease diagnosis, as assertion consistent with clinical and pathological observations [1, 24, 49, 50]. In demonstrating significant differences between AD-DS and AD, they raise the possibility that several *APP* products could contribute to pathogenesis, possibly through different mechanisms. Importantly, they argue that investigations to define the APP product(s) responsible for pathogenesis in DS are essential and against assigning to any product a singular role. Studies in which each of several APP products are examined in rodent and human model systems will be necessary to clarify which products act, when they act, how they act and whether their actions contribute to AD in DS. In summary, our findings help to create a roadmap for studies to further explore the hypothesis and to decipher how an extra copy of the *APP* acts to cause AD in DS. We highlight possible approaches and speculate on what methods and reagents could be used to reduce *APP* expression in those with DS. Finally, we address near-term possibilities for preventing AD in DS that build upon the rationale that reducing *APP* products may prove effective even absent a full explication of pathogenesis.

Materials and Methods

Analysis of Human Brain Tissues

The postmortem human brain tissues from the mid-frontal cortex were obtained from the Banner Sun Health Research Institute (Phoenix, AZ; SHRI), UCSD-ADRC (La Jolla, CA), and UCI-ADRC Brain tissue repository (Irvine, CA)(Table 1). Controls (ND: non-demented) ranged in age from 58 to 102 (average: 83 years), AD cases from 64 to 94 (average: 85 years), and AD-DS cases from 45 to 70 (average: 53 years). Though younger on average than the ND and AD cases, the ages for AD-DS cases correspond to those at which people with DS are at markedly increased risk for AD; this is borne out by neuropathological staging (Table 1). As referenced, ~50% of people with DS are diagnosed with AD-DS at age 56 [51] – two or three decades younger than for sporadic AD, in which disease is most common in the 75 to 84 (48%) and 85 and older (38%) age cohorts [52].

In all cases, the staging of neurofibrillary pathology was via Braak and Braak (1991). For SHRI cases: 1) non-demented control cases were without dementia or parkinsonism during life and without a major neuropathological diagnosis. Cases with mild cognitive impairment (MCI) were grouped with control cases, as were cases with incidental Lewy bodies, essential tremor, restless legs syndrome, and other tremor disorders. 2) Diagnosis of AD was defined as intermediate or high NIA Reagan criteria [53]. Neuropathological classification of plaques was based on CERAD neuritic plaque frequency at maximum density in the neocortex (0, sparse, moderate, frequent, or 0–3) [54]. For the ADRC cases, the pathological staging of amyloid used the Thal Phase (0–5) to score the hierarchical deposition of Aβ-containing plaques - i.e. a measure of amyloidosis not a measure of neuritic plaques- in the following regions: hippocampal sectors CA1, CA2, CA3, and CA4, the outer and inner portion of the molecular layer of the fascia dentata, the fascia dentata granule cell layer, the layers of the entorhinal cortex, all neocortical areas, the cingulate gyrus, the basal nucleus of Meynert, the hypothalamus, the thalamus, the basal ganglia, the subthalamic nucleus, the midbrain, the pons, the medulla oblongata, and the cerebellum [55].

Two groups of cases with DS were included in this study from the UCI-ADRC Brain tissue repository: with and without AD dementia (AD-DS and DS respectively). AD-DS dementia status classification followed comprehensive assessments including medical history, neurological examination, and neuropsychological evaluation with particular attention given to other health co-morbidities or neuropsychiatric conditions that might cause or mimic dementia (e.g., thyroid dysfunction, sensory impairment, depression, seizures, medication side effects, and other systemic illnesses). The diagnosis of dementia in AD-DS was based upon a consensus opinion from two or more independent raters after a comprehensive evaluation of existing records and data. Participants were classified as demented if there was a history of progressive memory loss, disorientation, and functional decline over at least six months. One DS case with partial trisomy 21, reported previously [28] was included in the study. Neuropathological classification of amyloid was based on amyloid plaque stages – 0, A, B, and C [56].

The frozen tissues were homogenized in a two- to three-times volume of RIPA buffer (25 mM Tris-HCl pH 7.5, 150mM NaCl, 1% NP-40, 1% sodium deoxycholate, 0.1% SDS) containing Halt™ Protease and Phosphatase Inhibitor Cocktail (Thermo Fisher Scientific) using the Bullet Blender (Next Advance). After centrifugation for 15 min at 13,000 rpm at 4°C, the supernatant was collected for biochemical analyses. For quantification of fl-hAPP and hCTFs, 30 μg of total lysate was loaded on 10% Bis-Tris Criterion gels or 16.5% Tricine gels (BioRad). Proteins were transferred onto polyvinylidene fluoride (PVDF) membranes. After boiled in 1xPBS for 5 min, membranes were blocked with 5% milk at RT for 1hr and blotted using antibodies against hAPP for detection of fl-hAPP and hCTFs (Y188, 1:2000, Abcam). For separation of hCTFs at higher resolution, 16.5 % tricine gels (BioRad) or 16% tricine gels prepared using SE660 Tall Standard Dual Cooled Vertical Protein Electrophoresis Unit (Hoefer) were used. For the analysis of expression levels of enzymes, the following antibodies were used: anti-Nicastrin antibody (D38F9, 1:1000, Cell Signaling), anti-PEN2 antibody (D6G8, 1: 1000, Cell Signaling), anti-Presenilin 1 antibody (D39D1, 1:1000, Cell Signaling), anti-Presenilin 2 antibody (D30G3, 1:1000, Cell Signaling), anti-ADAM10 antibody (#14194, 1:1000, Cell Signaling), anti-BACE1 antibody (MAB931, 1:250, R&D systems) and anti-BACE2 antibody (ab27045,1:1000, Abcam). For total and pT212-Tau analysis, protein lysates were resolved using 8% hand-casted Tris-polyacrylamide gels or 10% Criterion™ XT Bis-Tris Protein Gels (BioRad) and detected using anti-Phospho-Tau (Thr212) antibody (44–740G, 1:1000, Thermo Fisher Scientific), or anti-Tau antibody (Tau-5, 1:5000, Abcam). Anti-β-Actin (A5441, 1:5000, Sigma), anti-GAPDH (MAB5718, 1:10,000, R&D SYSTEMS), and anti-β-Tubulin (T0198, 1:5000, Sigma) antibodies were tested; the anti-Actin antibody was used as an internal control for quantification. After incubation with secondary antibodies, signals were detected using enhanced chemiluminescence (BioRad) and analyzed using a ChemiDoc XRS+ imaging apparatus (BioRad) and Image J. Quantitation of western blot (WB) images used densitometry for exposures in the linear range of detection.

Analysis of Mouse Brain Tissues

Dp16 mouse model of DS.—*Dp(16)1Yey/+* (Dp16) mice [57] and their 2N control littermates were used. Dp16 mice contain a duplication orthologous to human chromosome 21q11-q22.3 and carry 113 genes orthologous to genes on HSA21. Dp16 mice demonstrate behavioral deficits [57–59], and impaired hippocampal-mediated learning and memory [58]. Dp16 mice were maintained by crossing females to male (C57BL/6J × C3H/HeJ) F1 mice (B6C3). Diploid (2N) littermate mice on the same background served as controls. To produce Dp16 mice harboring only 2 mouse *App* alleles (i.e. Dp16:*App*++-), Dp16 mice were crossed with 2N mice lacking one copy of *App* (i.e. 2N:*App*+- mice) [60] on the same strain background. The genotype of all animals was confirmed by polymerase chain reaction (PCR). For genotyping, tail samples were used to extract genomic DNA. A protocol was used to amplify the HPRT insertion which is only found in Dp16 mice along with amplification of the IL-2 gene as an internal control. The primer sequences used for HPRT were: fwd: 5'-AGGATGTGATACGTGGAAGA-3'; rev: 5'-CCAGTTTCACTAATGACACA-3'; while the primers for IL-2 were: fwd: 5'-CTAGGCCACAGAATTGAAAGATCT-3'; rev: 5'-GTAGGTGGAAATTCTAGCATCATCC-3'. For m*App* the primers were fwd: 5'-

AGAGCACCGGGAGCAGAGCG-3'; rev: 5'- AGCAGGAGCAGTGCCAAGC-3'. For the *Neo* insert the primers were: inNeo F1: 5'-ATGGATACTTTCTCGGCAGGAGC-3'; inNeo R1: 5'- GAGGCTATTCGGCTATGACTGGG-3'.

All animals were maintained and bred according to standard procedures. Mice were housed 2 to 5 per cage with a 12 hr light-dark cycle and *ad-lib* access to food and water. Mice for all studies used sample sizes targeted to detect statistically significant differences of ≥20%. Mice were 2, 4, 8, 12, 14, or 19–20 months of age for biochemical experiments; 4–6, 8–10, or 13–19 (mean 16) months of age for neuropathological experiments. The evaluation of m*APP* gene dose on biochemical and neuropathological phenotypes was carried out in a blinded fashion. Sacrifice was between 7 AM and 7 PM daily; best efforts were made to minimize suffering.

RNA extraction and real-time quantitative PCR (RT-qPCR) analysis—Total RNA was extracted from the mouse cortex, cerebellum, and hippocampus using the RNeasy Lipid Tissue Mini Kit (QIAGEN). Complementary DNA (cDNA) was synthesized using the High-Capacity cDNA Reverse Transcription Kit (Applied Biosystem). Total RNA (1 μg) was used as a template. RT-qPCR reaction was performed using PowerUp™ SYBR™ Green Master Mix (Applied Biosystem) with 10 ng of cDNA as a template. Eight genes (m*APP, Dyrk1a, Kcnj6, Synj1, Rcan, Bace2, Itsn, Sod1*) were analyzed to evaluate gene expression in the cortex of 2N and Dp16 mice at 4 and 19 months and cerebellum at 12 months. For validation of the NanoString analysis, an additional four genes (*Olfm3, Per1, Ctss, Psmg1*) were analyzed in the hippocampus at 4 months and four genes (*Aph1a, Samd4, Fxyd5, Psmg1*) in the hippocampus at 19 months. *Gapdh* was used as an internal control. Data was acquired using Applied Biosystems 7300 Real-Time PCR System (Applied Biosystem) and analyzed using Applied Biosystems 7300 Fast SDS Software (Applied Biosystems™).

Gene expression study using a NanoString AD panel—Alterations of gene expression among 770 AD-associated genes discovered in the AMP-AD consortium study [61] were examined using the nCounter mouse AD panel (NanoString Technologies). Briefly, total RNA was extracted from the hippocampus of 2N and Dp16 mice at 4 and 19 months using the methods outlined above. 100ng of total RNA was used for hybridization to the capture and reporter probes following the manufacturer's protocol. Image acquisition was done using the nCounterSPRINT profiler (NanoString Technologies). The data was processed and analyzed using nSolver and nCounter Advanced Analysis 2.0 software (NanoString Technologies). Nine housekeeping genes were used for normalization. Differentially expressed genes between the groups were selected with a p-value of <0.05 (adjusted p-value, t-test).

Immunoblot analysis of mouse brain—Cortex and hippocampus of 2N and Dp16 mice at 4 and 19 months were dissected and homogenized in a three- to five-fold volume of RIPA buffer (25mM Tris-HCl pH 7.5, 150 mM NaCl, 1% NP-40, 1% sodium deoxycholate, 0.1% SDS) containing Halt™ Protease and Phosphatase Inhibitor Cocktail (Thermo Fisher Scientific) using the Bullet Blender (Next Advance). After centrifugation at 13,000 rpm for 15min at 4°C, the supernatant was used for immunoblot analysis. 45 μg of total protein was loaded on 4–12% NuPAGE Bis-Tris gels and blotted onto PVDF membranes.

Membranes were boiled in 1xPBS for 5 min followed by blocking with 5% milk for 1hr at RT. fl-mAPP and mCTFs were detected with antibodies against hAPP (Y188, 1:2000, Abcam), which cross-reacts with mAPP, followed by incubation with secondary anti-Rabbit IgG antibodies tagged with horseradish peroxidase (1:5000, Santa Cruz Biotechnology). The Anti-BACE1 and BACE2 antibodies and anti-pT212 and anti-total Tau antibodies listed above were used for the analysis of enzymes, and total and pT212-Tau analysis, respectively. Signals were visualized with enhanced chemiluminescence and analyzed with a ChemiDoc XRS+ imaging apparatus (BioRad). Anti-β-tubulin antibody (T0198, 1:5000, Sigma) or anti-GAPDH antibody (MAB5718, 1:10,000, R&D systems) was used as a loading control. WB images were quantified using densitometry of exposures in the linear range of detection.

Immunohistochemistry, immunofluorescence, and image analysis—To evaluate the effects of *APP* dose on neurodegeneration, tissue from Dp16 and 2N control mice was serially sectioned every 40 μm in the coronal plane using a vibratome. Sections were incubated overnight at 4°C with antibodies against the pan-neuronal marker NeuN (1:1000, Millipore), the cholinergic cell marker choline-acetyl transferase (ChAT, 1:1000, Millipore) or the catecholaminergic cell marker tyrosine hydroxylase (TH, 1:1000, Millipore). pTau (PHF-1, 1:10,000, Courtesy of P. Davies), and a microglial marker (IBA1, 1:1,000, Wako Laboratories) were employed to detect tau pathology and microglial activation, respectively. Primary antibody incubation was followed by biotinylated secondary incubation (1:1000, Vector Laboratories), Avidin-Biotin Complex (ABC Elite, 1:200, Vector), and developed by incubation with diaminobenzidine.

The numbers of NeuN (entorhinal cortex; layer 2/3), ChAT immunoreactive (medial septum) and TH immunoreactive (locus coeruleus) neurons were estimated using unbiased stereological methods [62]. Sections containing the entorhinal cortex, medial septum, or LC were outlined using an Olympus BX51 microscope running StereoInvestigator 8.21.1 software (MicroBrightField). The average coefficient of error for each region was 0.09. Sections were analyzed using a 100X 1.4 PlanApo oil-immersion objective. A 5-μm-high dissector allowed for 2 μm top and bottom guard zones. For the medial septum grids were set as previously described [63]. For densitometry analysis of PHF-immunoreactivity, images of the cortex above the rostral hippocampus were taken under identical conditions using a 100 X 1.4 oil-immersion objective on an Olympus BX50 microscope running custom-written code in MatLab. One section was re-analyzed at the beginning and end of the imaging session each day to control for light intensity changes.

To probe for Rab5, sections were incubated in sodium citrate buffer (10mM sodium citrate 0.05% tween 20, Ph6.0) (Thermo Fisher Scientific) at 90° for 20 minutes. After antigen retrieval, sections were washed 3x for 5 min with Tris buffered saline (TBS) (100mM TBS, 137mM NaCl, pH 7.8) and permeabilized with 0.1% Triton X-100 (TX) (Thermo Fisher Scientific) for 15min. Non-specific binding was blocked with 2% normal goat serum in TBS with 0.1% TX for 30 min before overnight incubation in 5μg/mL anti-Rab5 (Clone C8B1, Cell Signal Technologies) primary antibody along with the primary antibody for cholinergic cell marker choline-acetyl transferase (CHAT; 1:1,000; Millipore, Temecula, CA). After washing 3x in TBS with 0.1% TX and blocking with 2% normal goat serum (Vector Laboratories) in TBS with 0.1% TX for 30 min, sections were incubated in

ALEXA555 conjugated anti-rabbit secondary (Invitrogen) at a dilution of 1:500. Cell nuclei were counter-stained with DNA dye TOPRO3 (Invitrogen) by incubating at a concentration of 1μM for 15 minutes. An investigator blinded to genotype examined randomly selected fields for analysis. Confocal micrographs were obtained with Leica DMi8 equipped with a white light laser source for fluorescence measurements, using 551 and 630 nm excitation wavelengths for ALEXA555 and TOPRO3, respectively. Optical sections (58.13μm x 58.13μm) were taken using HC PL APO CS2 100x/1.40 oil immersion objective and processed using Leica LAS X Software (Germany) and analyzed using ImageJ particle analysis (NIH, USA).

To probe for GFAP, sections were washed 3x for 5 minutes with TBS and permeabilized with 0.1% TX for 15 min. Non-specific binding was blocked with 2% normal goat serum in TBS with 0.1% TX for 30 minutes before overnight incubation in 1μg/mL anti-GFAP (Agilent/Dako) primary antibody. After washing 3x in TBS with 0.1% TX and blocking with 2% normal goat serum in TBS with 0.1% TX for 30 minutes at RT, sections were incubated in biotinylated goat anti-rabbit secondary (1:1000, Vector Laboratories) for 1 hour at RT. Signal amplification and visualization were accomplished with 1-hour incubation in Avidin-Biotin Complex (ABC Elite, 1:200, Vector), followed by incubation with diaminobenzidine (DAB, Vector). Stereological analysis of the numbers of GFAP-immunoreactive cells in the entorhinal cortex (Allen Brain Atlas) was conducted with Stereologer ver 11.0 (SRC Biosciences); counts were conducted on a Nikon E600 with 100x/1.25NA. The number of GFAP+ cells was quantified in every 12th section (with 480 μm between sections) through the entire anteroposterior extent of the entorhinal cortex. We used a counting frame of 1000 μm^2 with step lengths 316 μm x 316 μm. Cell counts are represented as the number of cells per mm^3 and data collection and statistical analysis were conducted with groups blinded.

MSD assay of human and mouse brain tissue

Concentrations of Aβ38, 40, and 42 were measured using the V-PLEX Aβ Peptide Panel (4G8: Meso Scale Discovery) following the manufacturer's instructions. 250 μg of mouse brain lysate and 350 μg of human lysate were analyzed in a volume of 25 μl. Data were obtained using the MESO QuickPlex SQ 120 and analyzed using DISCOVERY WORKBENCH 3.0 (Meso Scale Discovery). The pg concentration of Aβ species in 25 μl was converted to pg/ml values for determining mean values and for comparison of samples. The protein concentrations (pg/mg) in lysates were also calculated.

Experimental Design and Statistical Analysis

All analyses were performed using GraphPad Prism (version 8.0) software, and values in the Figures are expressed as means ± SEM. For the statistical analyses of human protein lysate, all experiments were in performed in triplicate and analyzed using, either one-way analysis of variance (ANOVA) followed by Dunn Multiple comparison test or two-way ANOVA with Tukey's multiple comparisons performed, depending on the categories of the factors. For analysis of the mouse model, we performed either a t-test or Mann Whitney test. All IHC experiments and analysis were performed blind-coded, and values were compared using one-way analysis of variance (ANOVA) with Dunnett's *post-hoc* test. Each type of statistic is specified in each Figure legend. Adjusted p-values are reported for specific comparisons

in the Preliminary Findings. The differences were significant if the p-values were less than 0.05. A one-way ANOVA analysis was performed for PMI. There were no significant differences between groups for PMI when evaluating the full data set. Out of an abundance of caution, outlier analysis was performed using GraphPad Prism 8. ROUT outlier analysis identified 5 cases which outliers for their respective PMI; namely X5783 (ND, 36 hrs); ND:X5302 (ND, 72 hrs); X5812 (AD, 16 hrs); X5799 (AD, 15 hrs); X5583 (AD, 14 hrs). The inclusion of these cases did not influence the conclusion of the statistical analyses.

Preliminary Findings

APP and Its Cleavage Products in DS Brains: Comparisons to AD and ND

Gene dose-dependent increases in fl-hAPP in AD-DS and DS.: To evaluate hAPP expression and processing in brains of DS and AD-DS, and to compare the findings to those in other populations, we examined cases of non-demented (ND) populations without DS (male: n=12, age 74–94; female: n=8, age 58–102), DS cases with AD (AD-DS; male: n=4, age 46–70, female: n=7, age 45–62), DS without AD (DS; female: n=4, age 42–62) and AD without DS (AD; male: n=10, age 64–89; female: n=11, age 80–94). The ages for DS and AD-DS cases correspond to those at which people with DS are at markedly increased risk for AD, as supported by neuropathological staging (Table 1). Approximately 50% of people with DS are diagnosed with AD-DS at an age that is two or three decades younger than for sporadic AD [51], explaining the use of NDs in this age range for both the AD and DS cases. The demographics of cases are given in Table 1. *APOE* allele status was recorded in all AD cases, and in all but one ND; the E3 allele was the most frequent, with only one E4 homozygous AD female. Of a total of 16 DS cases, *APOE* status was recorded in 9. As in the general population, the E3 allele was most frequent; none were E4 homozygotes.

Protein lysates were prepared from the frozen frontal cortex. fl-hAPP and hCTFs levels were analyzed by SDS-PAGE and western blots. Anti-Tubulin, anti-Actin, and anti-GAPDH antibodies were tested as loading controls. Anti-actin was selected for quantification of human samples since this antibody showed the most consistent pattern of signals with respect to the amount of total protein loaded per lane (Figure 1a, d). We first analyzed the samples in a sex-matched manner. There was no consistent difference in the banding pattern for fl-hAPP when comparing AD-DS, DS, and AD with ND (Figure 1a, d). However, consistent with increased *APP* dose, there was an increase in the amount of fl-hAPP in DS independent of the diagnosis of AD. In AD-DS, significant differences were observed in both males and females (Figure 1b, e, Table S1). In males, fl-hAPP averaged ~2-fold in comparison to ND ($p = 0.0119$) (Figure 1b); in both AD-DS and DS females the ratios were increased to ~1.5-fold relative to ND ($p = 0.0115$) (Figure 1e; Table S1). In AD cases, the levels of fl-hAPP in males and females varied when normalized to the actin control, but neither group differed significantly from ND (male $p > 0.9999$, female $p=0.4467$) (Figure 1a, b, d, e, Table S1). These data are evidence that fl-hAPP was increased to levels proportional to gene dose in both male and female adults with AD-DS and DS.

hCTF levels in AD-DS and DS.: hCTFs were detected at apparent molecular weights between ~11 and 17 kDa in all the human postmortem brain samples (Figure 1a, d). There was variability in the levels and relative intensity of longer (i.e., pC99 and C99; also known

as β-CTFs) versus shorter (pC89, C89, pC83, C83; α-CTFs) forms, across samples. hCTFs were increased in both males and females with DS, with or without AD, in comparison to ND (Figure 1a, c, d, f). In AD-DS males, compared to ND males, there was a significant ($p = 0.0095$) ~ 2.5-fold increase in hCTFs relative to actin. There was also a significant ~ 2.5-fold increase in AD-DS males compared to AD males ($p = 0.0203$) (Figure 1a, c). However, this increase was not significant compared to fl-hAPP ($p > 0.9999$) (Table S1; Figure S1a). Increases in hCTFs were also detected in both AD-DS and DS females. Compared to female ND, hCTFs were approximately 5-fold increased in AD-DS and DS relative to actin (AD-DS, $p = 0.0149$, DS, $p = 0.0307$), and female AD-DS cases had significantly increased hCTFs compared to female AD cases (~2.8-fold, $p = 0.0312$) (Figure 1 d, f). Moreover, the ~ 3- to 4-fold increases with respect to fl-hAPP (Figure S1b) were significant [ND: CTF/APP = 1.070 ± 0.1394 (average ± SEM); AD-DS = 2.938 ± 0.3911 [p=0.0391]; DS: 3.789 ± 0.7698 [p=0.0493] (values were normalized to the ND average hCTF/fl-hAPP) (Table S1). In those with AD but not DS, the levels for hCTFs varied in males and females (Figure 1a, d), but on average showed no significant difference relative to ND when normalized to actin (Figure 1c, f) or in proportion to fl-hAPP (Figure S1a, b, Table S1). These data demonstrate that while the increase in hCTFs in the brains of people with AD-DS was present in both males and females, in females the increases exceeded those predicted based on *APP* dose, as reflected in the levels of fl-hAPP.

Increased Aβ peptide levels in AD-DS, DS, and AD: comparison to ND.: We measured concentrations of Aβ38, 40, and 42 in brain lysates using the V-PLEX Aβ Peptide Panel 1 (4G8: Meso Scale Discovery). Table S2 reports on the absolute levels of each Aβ peptide in ND, AD-DS, DS, and AD samples in the assay. Though individual samples varied, increases in average absolute levels relative to the ND values were detected for each of the Aβ peptides examined in each set of DS samples (Figure 1g–i). With respect to Aβ42 the increases in AD-DS males and females with AD-DS and DS averaged ~ 45 to ~100-fold the ND values (absolute values: ND = 18.73 ± 12.08 pg/ml (average ± SEM); male AD-DS = 856.0 ± 143.6 [p vs ND = 0.0002]; female ND= 6.339± 3.168; female AD-DS= 658.1 ± 258.1 [p vs ND = 0.0017]; female DS= 603.1 ± 87.30 [p vs ND = 0.0028])(Table S2). These values were increased in proportion to fl-hAPP levels by ~ 20-fold in AD-DS males and ~40-fold in AD-DS and DS females (Table S3); all increases with respect to fl-hAPP were statistically significant (statistics: vs sex-matched ND; AD-DS males $p = 0.0059$; AD-DS females $p = 0.0109$; DS females $p= 0.0094$) (Figure S1c, Table S3). When comparing ND males versus ND females, or AD-DS males versus AD-DS females, Aβ42 did not show statistically significant differences in absolute levels (for ND, $p = 0.2463$; for AD-DS, $p = 0.3152$) (Figure 1g); the same comparisons between sexes failed to show significant differences when expressed with respect to fl-hAPP (for ND, $p = 0.2303$; for AD-DS, $p = 0.2544$) (Figure S1c; Table S3). Statistically significant increases of Aβ40 were also observed in male and female AD-DS (Figure 1h, Table S2); relative to sex-matched ND: ~42-fold in male AD-DS ($p = 0.0214$), ~45-fold in female AD-DS ($p = 0.0103$) (Figure 1h, Table S2). Aβ40 levels were also significantly increased in proportion to fl-hAPP; relative increases to the sex-matched ND: ~15-fold in male AD-DS ($p = 0.0214$), ~50-fold in female AD-DS ($p = 0.0103$) (Figure S1d, Table S3). Comparing males and females with AD-DS, no statistically significant difference was observed in the absolute values of Aβ40 ($p >$

0.9999) or in proportion to fl-hAPP levels (p = 0.7360). Lesser but significant increases of ~10-fold were detected in DS females (p = 0.0433 versus female ND) (Figure 1h, Table S2); for these subjects, the increase in Aβ40 with respect to fl-hAPP was not significant (p = 0.2534, Figure S1d, Table S3). For Aβ38 relative to the sex-matched ND, the concentration was increased in both male AD-DS (p = 0.0045) and female AD-DS (p = 0.0012) (Figure 1i), averaging ~30-fold in males and ~50-fold in females (Table S2). Lesser increases were present in DS females relative to ND females; they averaged 19-fold (Figures 1i, Table S2) but they were not statistically significant (p = 0.1068 relative to female ND). While the increase in Aβ38 relative to fl-hAPP was statistically significant for AD-DS males (p = 0.0154), this was not the case for AD-DS or DS females (p = 0.0601, p > 0.9999, respectively) (Figure S1e, Table S3).

We also measured Aβ peptide levels in those with sporadic AD. Aβ42 levels were increased in both males (~15-fold enrichment) and females (~30-fold) (Figure 1g. Table S2); while in males the increase was significant with respect to the sex-matched ND (p = 0.0061), in females the very strong trend failed to reach statistical significance (p = 0.0608). However, in neither males nor females were the increases significantly greater than predicted by fl-hAPP in comparison to the sex-matched ND (male, p = 0.161; female, p = 0.1598) (Figure S1c, Table S3). Levels of Aβ42 in AD did not show significant differences between males and females with respect to concentration (p = 0.7013) or with respect to fl-hAPP (p = 0.1964). Aβ40 levels were increased in AD males and females by ~4-fold, a result that was significant in males (p = 0.0045) but not in females (p = 0.3908) (Figure 1h, Table S2). Relative to fl-hAPP neither the increases in males nor females were significant (Figure S1d; Table S3). For Aβ 38 levels, while average increases of ~ 4- to 9-fold were detected in AD males and females, respectively (Figure 1i, Table S2), the increases were not significant as compared to sex-matched ND (males p = 0.7777, females p = 0.0596, respectively) (Figure 1i) or with respect to fl-hAPP (Figure S1e, Table S3).

Comparing AD-DS versus AD, both males and females with AD-DS had much higher levels of all three Aβ species than in AD males and females (Table S2). Indeed, a several-fold increase was documented for each Aβ species (~3-fold for Aβ42, ~11-fold for Aβ 40 and ~6-fold for Aβ38; Table S2); the increases in Aβ42 and Aβ40 in AD-DS significantly exceeded those predicted by fl-hAPP (Table S3). These data are evidence that the AD-DS brain differs from the AD brain in much larger increases in Aβ species.

The ratio of Aβ42 to Aβ40 provides indirect estimates for the activity of γ-secretase, as well as the regulation of Aβ metabolism and clearance [37, 64, 65]. In an earlier study, the kinetics of synthesis and clearance used the SILK method, which radiolabels newly synthesized proteins and follows their appearance over time in CSF [66]. While similar kinetics were observed for Aβ42, Aβ40, and Aβ38 in patients without amyloid plaques, in those with plaques there was an increase in the fractional turnover rate for Aβ42 relative to Aβ40 and Aβ38 [66]. Positive correlations for an increase in the ratio of Aβ42/Aβ40 turnover rates with plaque load and plaque growth rate combined to suggest that Aβ42 is more readily incorporated into amyloid plaques than Aβ40 or Aβ38 [66–68], a posit also consistent with the decrease in the CSF Aβ42/40 ratio in AD [69].

We explored the hypothesis that as for AD, due to sporadic, late-onset disease as well as familial AD (FAD), in AD-DS there would also be an increase in the Aβ42/Aβ40 ratio [70, 71]. As expected, in males and females with sporadic AD the Aβ42/Aβ40 ratio was significantly increased compared to the sex-matched ND (males $p = 0.0014$, females $p = 0.0024$) (Figure S1f). In females with DS, a significant increase in the Aβ42/Aβ40 ratio was also observed ($p = 0.0291$). However, concomitant large increases in both Aβ42 and Aβ40 in AD-DS males and females reduced the ratio (Figure 1g, h, Figure S1f, g). The Aβ42/Aβ38 ratio was also significantly increased in males and females with sporadic AD compared to the sex-matched ND (males $p = 0.0008$, females $p = 0.0209$) (Figure S1g). Females with DS also showed a significant increase in Aβ42/Aβ38 ($p = 0.0353$); however, relatively larger increases in Aβ38 in males and females with AD-DS blunted this ratio (Figure 1i, Figure S1f, g). Thus, while in AD increases in the Aβ42/40 and Aβ42/38 ratios were confirmed, the concomitant and greater increases in Aβ40 and Aβ38 precluded this demonstration in AD-DS.

APP and Its Cleavage Products in Partial Trisomy and Mosaic DS.: To further evaluate the impact of *APP* gene dose in AD pathogenesis in DS, we examined fl-hAPP, hCTFs, and Aβ peptides in the brain lysate of an individual with partial trisomy 21 (PT-DS) (Table 1). In extremely rare cases [72–74], only a portion of HSA21 is present in excess [75], resulting in PT-DS. This person was the subject of a previous report of PT-DS in which the genome was shown to harbor the normal 2 copies of h*APP.* While demonstrating many of the clinical features of DS, molecular analysis revealed an increase in copy number for only 18.8Mb, extending from position 28.12 Mb to the telomere of HSA21; excluded from the duplication was a 1.95Mb region containing *APP* (26.17 Mb). This and another report highlighted the important role of h*APP* gene dose in AD pathogenesis in DS [27, 28] because neither case manifested declining cognition in old age or the pathology of AD at postmortem examination. This male PT-DS reported by Doran *et al.* [28] was a 65-year-old man followed over 7 years during which time normal plasma levels of Aβ40, and undetectable plasma levels of Aβ42, were documented. On PiB-PET scanning he registered SUVr values lower than for AD and typical DS subjects and that was similar or lower than healthy controls. Postmortem exam showed the absence of neuritic plaques except for trace amounts in CA1 and NFTs judged to be Braak stage III [28]. The brain lysate from this patient demonstrated, as expected, the typical banding pattern for fl-hAPP with no increase in the level of fl-hAPP, in the levels of Aβ42, Aβ40 or Aβ38, or the ratios of Aβ42/40 or Aβ42/38 (Figure 1a, b, g–i; Figure S1c–g). Surprisingly, there was a marked increase in the levels of hCTFs (Figure 1c) with values comparable to those in males with AD-DS; indeed, the ~2:1 ratio of CTFs to fl-hAPP was greater than seen in AD-DS males (Figure S1a).

Another rare type of DS results from mosaicism for HSA21 (~2% of total cases) in which cases the extra chromosome is present in some but not all cells, the percent of which may vary across tissues [14]. In a single female case of mosaic DS examined herein (aged 48, Plague Stage B, Braak Stage III) (Table 1) we expected to find that the extent to which neurons harbored the extra chromosome would be reflected in increases in fl-hAPP and its products. However, whereas fl-hAPP was not increased, there was an increase in hCTFs and the ratio of hCTFs to fl-hAPP; the values recorded approximated those in DS and AD-DS

females (Figure 1d–f, Figure S1b). Consistent with the presence of amyloid plaques on postmortem exam, we detected an increase in the absolute levels of Aβ42 and Aβ40, but not Aβ38 (Figure 1g–i). The increase in Aβ42 and the ratio of Aβ42/40 (Figure S1f) were equivalent to those in DS and AD-DS females, while the Aβ42/38 ratio exceeded the same ratio in DS and AD-DS females (Figure S1g).

Summarizing the data for DS, the levels of fl-hAPP and its products are impacted in the context of full trisomy for HSA21 as well as in the cases of PT-DS and mosaic DS examined herein. These findings point to *APP* dose as one factor for regulating the levels of fl-hAPP and suggest that increased *APP* dose influences other processes, possibly including processing and clearance of fl-hAPP. Given the data for the mosaic DS case, the further possibility is raised that aneuploidy in a minority of cells may induce changes in hAPP products.

Evidence for Sex Differences in hAPP processing in DS: studies in AD-DS, PT-DS, and DS-mosaic cases.: Our initial analysis (Figure 1a–f and Figure S1a, b) indicated that male and female cases with AD-DS differ in the levels of CTFs. To further address possible sex effects, we reexamined the levels of fl-hAPP and hCTFs in male and female ND and AD-DS cases on the same blot (Figure 2a–g). When normalized to the actin control and expressed relative to the male ND, the female ND cases showed a slight increase in fl-hAPP. There was a significant increase in fl-APP in the female AD-DS cases compared to both ND males (p-value = 0.0029) and ND females (p-value = 0.0223; Figure 2b). Male AD-DS cases also showed an increase, albeit smaller than shown in Figure 1b (1.6-fold vs 2.1-fold the ND male control) and insignificant using a two-way ANOVA followed by Tukey post hoc analysis. Note, however, that comparing male ND to male AD-DS there was a significant difference when evaluating this data using a one-way ANOVA followed by Dunn's multiple comparison post hoc test (p-value = 0.0375). The increases in both male and female AD-DS thus approximated *APP* dose. There was no significant difference for the sex and genotype interaction (two-way ANOVA, p=0.5148) (Figure 2a, b). On the other hand, evaluation of hCTFs in female AD-DS compared to male AD-DS cases revealed a significant difference (post-hoc Tukey's multiple comparisons test, p = 0.0217), as well as for the sex and genotype interaction (two-way ANOVA, p= 0.0230) (Figure 2a, c). Thus, while the increase in AD-DS males were ~2.5-fold the ND males, for AD-DS females it was ~ 4-fold the ND females. After expressing the level of hCTFs with respect to fl-hAPP, the difference in male and female AD-DS was again apparent. While for male AD-DS there was no significant difference relative to ND subjects, the increase in female AD-DS was significant relative to both ND females and ND males (two-way ANOVA followed by post-hoc Tukey's multiple comparisons test, female AD-DS vs female ND: p = 0.0024; female AD-DS vs male ND p= 0.0158) (Figure 2d).

The enzymatic processing of fl-hAPP leads to the production of hCTFs of different molecular weights [76]. To better understand fl-hAPP processing in DS we evaluated the distribution of hCTF isoforms, quantifying shorter bands, corresponding to α-hCTFs (i.e., pC89, C89 plus pC83, C83) and longer ones, corresponding to β-hCTFs (i.e., pC99 and C99). The increase in hCTFs in female AD-DS was due to increases in both shorter (α-hCTFs; Figure 2e; p-value < 0.0001) and longer forms of hCTFs (β-hCTFs; Figure

2f; p-value < 0.0001). In males the, the increases relative to ND cases was only significant (p-value = 0.0444) for the shorter forms of hCTFs (Figure 2e, f). The ratio between shorter and longer hCTFs showed no significant differences comparing AD-DS to ND or comparing males to females (Figure 2g). To further characterize the distribution of hCTF fragments in samples, and explore the findings for hCTFs in the PT-DS and DS-mosaic cases, we analyzed a representative subset of AD-DS cases, and the PT-DS and DS-mosaic cases, using 16% tricine gels (Figure S2a–d). The PT-DS and DS-mosaic cases demonstrated a relatively larger fraction of α-hCTFs as compared to β-hCTFs (Figure S2a–d). Finally, we also compared AD-DS to AD by examining CTFs in AD cases (Figure S2e–h). No significant differences in the relative levels of α-hCTF species, β-hCTF species, or in the ratio between α-/β-hCTF species were found in comparing AD cases to sex-matched NDs. In summary, sex-based changes in the levels of the hCTFs were seen in AD-DS, with increased levels of hCTFs in females with full trisomy as well as in the mosaic DS. While in AD-DS cases both α-hCTFs and β-hCTFs were increased, the PT-DS and DS-mosaic cases demonstrated greater increases in α-hCTFs.

Examining the levels of APP processing enzymes in AD, AD-DS, PT-DS, and DS-mosaic cases.: To further explore hAPP processing, and in particular, to ask if the increase in hCTFs in females with DS was correlated with changes in the levels of processing enzymes, we examined the relative levels of ADAM10, BACE1, and 2 and components of the γ-secretase complex, including presenilin (PSEN) 1 and 2, nicastrin, and presenilin enhancer (PEN) 2 (Figure S2i–k) [76]. Brain lysates were subjected to SDS-PAGE and immunoblotting with antibodies to each of the enzymes listed (Figure S2i–k). As compared to ND females, significant increases were present in AD-DS females in the average levels of BACE2 (3-fold the ND; p = 0.0439), Nicastrin (mature) (1.4-fold the ND; p = 0.0024), and PEN2 (1.5-fold the ND; p = 0.0255) (Figure S2i: one-way ANOVA followed by a multiple comparison test). Mature BACE1 levels showed a trend to an increase in AD-DS females compared to female ND cases; statistical significance was observed by t-test between AD-DS and ND females but not with ANOVA (p = 0.0567). There were no significant differences for protein levels in male AD-DS versus their ND controls for any of the proteins examined (Figure S2i, j). For proteins, whose levels were significantly different in female AD-DS versus ND cases we calculated the ratio of the protein versus fl-hAPP; no significant differences relative to fl-hAPP were seen for BACE2, the mature forms of BACE1 and nicastrin or PEN2. Nor did AD-DS males show a difference (Figure S2k). We noted, however, that in the DS Mosaic case increases with respect to actin and relative to ND were detected for BACE2, nicastrin, and PEN 2; moreover, mature BACE1 levels were also increased.

In summary, female AD-DS cases demonstrated differences relative to male AD-DS in the levels of proteins that contribute to the processing of APP via BACE and the γ-secretase complex. They are further evidence for sex-linked differences in AD-DS females. Nevertheless, whether and how the changes are linked to increased hCTFs in DS females is unclear. Remarkably, an extra copy of the *BACE2* gene located on HSA21 was correlated with a significant increase in the levels of the protein in the brains of females but not males

with AD-DS. Indeed, neither AD-DS males nor the PT-DS male had significantly increased levels of BACE2, though their genomes harbor an extra copy of *BACE2*.

The phosphorylation status of Tau at Thr212 (pT212) correlates with tau pathology.: Hyperphosphorylation of Tau and the presence of these species in neurofibrillary tangles is a hallmark in AD pathogenesis, a relationship defined in part by the Braak stage [56, 77, 78]. Table 1 reports the Braak stage determined in our cases. To extend our studies comparing AD with AD-DS we investigated the phosphorylation of Tau, specifically focusing on pT212. Thr212 is targeted for phosphorylation by DYRK1A, whose gene is also encoded on HSA21. In addition to tau, many substrates are targeted by DYRK1A, including APP and PSEN, raising interest in the possibility that DYRK1A may contribute to AD pathogenesis, especially in the context of DS [13]. Thr212 is hyperphosphorylated in the AD brain; increases in phosphorylation are equal to or greater than other p-tau species in bands migrating at both greater than 65 kDa (high molecular weight [HMW] tau) and less than 65 kDa (low molecular weight [LMW] tau) [79]. Immunoblot analysis of levels of pT212 tau employed the same methods used for APP. pT212 tau was detected as a set of prominent bands at apparent molecular weights ranging from ~50 to 68 kDa, values consistent with earlier reports [79, 80]. Little if any pT212 tau was detected in either male or female ND cases (Figure 2 h–j, l). In AD-DS cases pT212 Tau was readily detected in both males and females, as compared to the sex-matched ND cases (males $p = 0.0001$, females $p = 0.0252$). Total Tau levels were detected using Tau 5, a pan-tau antibody that labels all six isoforms, with major bands ranging in apparent molecular weight from ~50 to 65 kDa. Interestingly, total Tau levels were also significantly increased in AD-DS cases compared to the sex-matched ND cases in both males and females (one-way ANOVA, followed by Dunn's multiple comparison test, males: $p = 0.0049$, females: = 0.0049) (Figure 2h, i, k, m). In contrast, we found little if any pT212 tau signal in the DS females without AD; total Tau levels were slightly but insignificantly increased. In the AD cases, the levels of pT212 tau were less than in AD-DS; there was a significant increase of pT212 in males ($p = 0.0041$) but not in females ($p = 0.2595$) (Figure 2j, l). Different from AD-DS, total Tau was not significantly increased in either male or female AD cases (males $p > 0.9999$, females $p = 0.3947$) (Figure 2k, m). Consistent with his Braak stage, the PT-DS case showed no detectable signal for pT212 tau. Thus, even though this person's genome carried three copies of *DYRK1A* there was no evidence of this activity with respect to pT212. In both PT-DS and DS Mosaic cases, no significant increase in total Tau was detected (Figure 2j, l).

To determine whether the increased levels of pT212 and total Tau in AD-DS cases (Figure 2h–m) showed a sex difference between males and females, representative samples of male and female ND cases (n=6 each), all the AD-DS cases (male n= 4, female n=7) and the PT-DS and DS-mosaic cases were run on the same gel. The levels of pT212 levels (Figure S2l, m) in AD-DS show no significant difference between males and females ($p = 0.6229$). Nor did we observe sex-based differences in total Tau expression in ND or AD-DS cases (ND $p = 0.3946$, AD-DS $p = 0.4804$) (Figure S2n, o). The levels of pT212 and total Tau in the PT-DS and DS-mosaic cases were equivalent to the ND cases. In summary, increases in pT212 and total tau point to additional significant differences between AD-DS and AD.

That the changes in AD-DS versus DS were correlated with increased Braak stage raises the possibility that increasing levels of pT212 and total tau mark increasing tau pathology during the progression of AD in this population.

Studies in the Dp16 mouse model of DS

Examining gene expression at the level of mRNA in the young and aged brain.: Measurement of APP products in postmortem human brain provides an important 'snapshot' of *APP* expression but does not inform as to how age impacts these values, or which can be implicated in neurodegenerative phenotypes. Examining *APP* gene dose effects in model systems complements human studies by documenting age-related changes, enabling comparisons between the levels of APP products in human and model brains, and deciphering the contributions of individual APP products to phenotypes. The Dp16 mouse model of DS has proven useful in examining relevant developmental and cognitive phenotypes [57] but a detailed evaluation of possible neurodegenerative changes has not been reported. The Dp16 model builds on the extensive synteny between the long arm of HSA21 and mouse chromosomes 16. It was created with chromosomal engineering and through partial duplication of mouse chromosome 16 carries an extra copy of all mouse chromosome 16 genes with a human homolog; in total, the Dp16 genome contains 105 genes also present on HSA21 [81]. m*APP* is present in three copies in these mice, as are several other genes with a possible role in the biology of AD, including *Dyrk1A*.

We first explored transcriptional alterations in Dp16 mice using the nCounter mouse AD panel (NanoString Technologies). This panel reports RNA levels of 770 target genes selected for relevance to AD based on postmortem studies of human AD samples [61, 82–84]. We assessed total mRNA extracted from the hippocampus of Dp16 and 2N mice at 4 and 19 months (n=3). Nine housekeeping genes (*Cnot10, Fam104a, Supt7l, Csnk2a2, Aars, Lars, Tada2b, Ccdc127, Asb7*) were used as internal controls to normalize data. Four comparisons of gene expressions were conducted: 2N versus Dp16 mice at 4 months; 2N versus Dp16 at 19 months, 2N at 4 months versus 9 months, Dp16 at 4 months versus 19 months. Results are shown with a cut-off at p-values < 0.05 and for changes that were increased or decreased $\geq 25\%$ (Table 2, Table S4). In comparing Dp16 to 2N, nine genes satisfied cut-off criteria at both 4 months and 16 months; at 4 months, 4 genes were decreased and 5 were increased. At 19 months only increases were detected. Three of the upregulated genes at both ages (*App, Syjn1,* and *Psmg1*) are encoded on the trisomic region; the increase in their RNA levels was in proportion to gene dose at both ages. Genes on other chromosomes were also significantly impacted in Dp16; interestingly, the RNA changes for these genes at 4 months showed no overlap with those present at 19 months (Table 2). Comparing RNA levels in 2N mice between 19 months and 4 months showed changes in transcripts for 12 genes that met cut-off criteria (Table S4), there were 4 decreases and 8 increases. We also detected 12 genes whose transcripts differed in Dp16 mice, comparing 19 months versus 4 months; in each case, the level of the RNA was increased and no genes on the duplicated segment met the cut-off (Table S4). To validate the findings, we selected four genes that showed significant changes across comparisons (*Olfm3, Per1, Ctss* and *Psmg1* [Dp16 versus 2N at 4 months]; *Apha1a, Smad4, Fxyd5* and *Psmg1* [Dp16 versus 2N at 19 months]) and performed RT-qPCR using cDNA synthesized with the total mRNA extracted from the hippocampus.

In the 4-month comparison, as predicted, expression of *Olfm3* and *Per1* showed significant decreases and *Ctss* and *Psmg1* showed significant increases (n=3, p-value = 0.05, one-tailed Mann-Whitney test; Figure S3a–d). In the 19-month comparison, *Apha1a*, *Fxyd5* and *Psmg1* showed the predicted significant increases (n=3, p-value = 0.05, one-tailed Mann-Whitney test; Figure S3e, g, h) but *Smad4* did not (Figure S3f). Thus, except for *Smad4*, these observations validated the findings from the nCounter mouse AD panel. Taken together, these data are evidence for transcriptional differences between Dp16 and 2N mice as well as for changes during aging in both genotypes.

Next, we separately analyzed the expression of m*APP* and seven genes encoded in the trisomic region that support neuronal function and/or are related to the pathology of AD: *Dyrk1a, Kcnj6, Synj1, Rcan1, Bace2, Itsn1, Sod1* [5, 11, 14, 76, 85, 86]. mRNAs extracted from cortex of 2N and Dp16 mice at ages 4 and 19 months were analyzed using RT-qPCR (n=4 and 5, respectively, at each age). We found significantly increased expressions of all eight genes duplicated in Dp16 mice compared to 2N mice at both 4 and 19 months (Figure 3a–h), with changes in each case approximating the increase in gene dose. At 19 months, 7 of the 8 genes showed statistically significant increases (Figure 3a–h); the increases were more variable with respect to gene dose (range: ~1.3 to 2.0-fold the 2N value). *Bace2* mRNA levels, while increased, failed to reach significance. To further characterize gene expression, and to examine a region not impacted in AD-DS, we also analyzed mRNA from the cerebellum of 12-month-old 2N and Dp16 mice. In the cerebellum, mRNAs for *App, Dyrk1a, Kcnj6, Synj1,* and *Rcan1* were increased significantly in Dp16 mice in comparison to 2N; the increases were equal to gene dose (*mApp, Dyrk1a*) or slightly greater than gene dose (*Kcnj6, Rcan1, Synj1*; ~2-fold 2N) (Figure S3i–m). While mRNA levels for *Bace2, Itsn1, and Sod1* were increased, the changes were not statistically significant (Figure S3n–p).

These data are evidence for age-related and regional differences in transcriptional regulation in Dp16 mice involving genes both within and distinct from the duplicated segment. Changes were registered in the expression of genes that encode products whose functions are linked to neurons and the biology of AD. Notably, increased levels of the mRNA for m*App* approximated the increase in m*App* dose across all brain regions and ages tested. The picture points to a widely disrupted transcriptional network whose contributions may impact many distinct molecular pathways during aging.

Increased levels of mApp and its products in young and aged Dp16 mice.: To examine age-dependent effects downstream from m*App* dose in the Dp16 mouse, we measured the levels of fl-mAPP and its products in the cortex at 2, 4, 16, and 19 months of age and in the hippocampus at 4 and 19 months. For analysis of mouse lysates, we used Tubulin or GAPDH as internal controls due to reproducibility and the correlation with the normalized total protein lysates. In cortex and hippocampus, the banding patterns for fl-mAPP and mCTFs did not appreciably differ between 2N and Dp16 mice; they corresponded to those in human samples expect that in mouse samples the relative amounts of shorter (α-mCTFs) versus longer fragments (β-mCTFs) was more uniform (Figure 3i), consistently demonstrating a predominance in α-mCTFs. fl-mAPP and its mCTFs were significantly increased in male Dp16 mice, as compared to 2N control, in cortex and hippocampus at 4

and 19 months of age; only the increase of fl-mAPP at 4 months in hippocampus failed to reach significance (Figure 3i–k). Only in the hippocampus of the Dp16 mouse at 19 months was the ratio of mCTFs/ fl-mAPP significantly increased compared to 2N mice ($p = 0.0066$, $p = 0.0415$; at 19 months and 4 months, respectively) (Figure S4a). Based on increased m*App* gene dose and given increased m*App* mRNA levels at age 4 months, we anticipated finding increased levels of fl-mAPP and its products at an early age. This expectation was confirmed for both fl-mAPP and mCTFs in the cortex at age 2 months wherein increases were present in Dp16 females compared to 2N females (Figure S5a–c). The increase in fl-mAPP (~1.3-fold the 2N level) was proportional to gene dose; for mCTFs, the levels were ~2-fold than those in 2N mice.

Mouse Aβ38, 40, and 42 were also measured in the cortex of 2N and Dp16 males at 4 and 19 months using the V-PLEX Aβ Peptide Pane 1 (4G8: Meso Scale Discovery, Rockville, MD). Aβ38 levels were under the detection limit in both Dp16 and 2N mice (data not shown). Aβ40 was increased in Dp16 versus 2N samples at both ages (Figure 3l). The increases relative to 2N mice were 1.8-fold at 4 months ($p=0.0286$) and 1.8-fold at 19 months ($p = 0.0079$). Interestingly, there was a significant increase of Aβ40 in both 2N and Dp16 at 19 months compared to 4 months (2N: 1.7-fold, $p = 0.0159$, Dp16: 1.6 -fold, $p = 0.0159$). Comparing Dp16 versus 2N samples, there was no significant change in the ratio of Aβ40/fl-mAPP at either 4 months or 19 months; however, the ratio in Dp16 mice at 19 months was significant with respect to both 2N and Dp16 mice at 4months (Figure S4b). A similar pattern was evident for Aβ42 (Figure 3m) but with Aβ42 present at much lower levels than for Aβ40. The increases relative to 2N mice were 1.4-fold at 4 months ($p=0.0286$) and 1.6-fold at 19 months ($p = 0.0079$). There was a significant increase of Aβ42 in both 2N and Dp16 at 19 months compared to 4 months (2N: 1.2-fold, $p = 0.0238$, Dp16: 1.6 -fold, $p = 0.0159$). Comparing Dp16 versus 2N samples, there were no significant changes for Aβ42/fl-mAPP at 4 months or 19 months. However, a significant increase was observed in Dp16 mice at 19 months vs Dp16 at 4months (Figure S4c). We calculated the ratio of Aβ42/40 in Dp16 and 2N mouse samples. There was no significant change between 2N and Dp16 at either 4 or 19 months of age, however, there was a small but significant decrease comparing Dp16 at 19 months versus 2N at 4 months (Figure S4d). In summary, both 2N and Dp16 mice showed age-dependent increases in Aβ40 and Aβ42 (Figure 3l, m). The increase in the ratios of Aβ40/fl-mAPP and Aβ42/fl-mAPP in old Dp16 mice (Figure S4a, b) is evidence suggesting accumulation of these species during aging albeit not beyond that predicted by *App* gene expression, as registered by fl-mAPP.

Next, we hypothesized that the sex effect seen for DS in humans would also be present in mice; fl-mAPP and mCTFs in male and female Dp16 and 2N mice were examined in the cortex at 8 and 14 months. At each age, there were strong trends for increases for both fl-mAPP and mCTFs in Dp16 males and females relative to 2N mice (Figure S5d–f). The increases in fl-mAPP were somewhat greater in females, but there were no statistically significant differences between male and female Dp16 mice for either fl-mAPP or mCTFs (at $p = 0.05$ threshold). Examining further the possible correspondence of sex differences in AD-DS, we also evaluated the levels of BACE1 and 2 in 8-month-old Dp16 and 2N mouse cortex. There was a modest increase in BACE2 in Dp16 versus 2N mice, but neither male nor female Dp16 mice differed significantly with respect to each other or 2N mice (Figure

S5g, i). However, as for females with AD-DS, female Dp16 mice showed a significant difference in mature BACE1 levels compared to male Dp16 mice by t-test, but not by ANOVA (p= 0.0009, p = 0.1748, respectively) (Figure S5h, j). There was no significant difference in the levels of immature forms of BACE1 (Figure S5h, k). Finally, as for DS samples, we examined the levels of the pT212 tau epitope in the cortex and hippocampus of male 2N and Dp16 at 4 and 19 months. Between 4 and 19 months, Dp16 samples showed on average an increase in pT212; relative to the 2N level at 4 months, the increase in cortex in Dp16 at 19 months was significant (Figure S5l, m). In hippocampus, the value in the 19 month Dp16 mouse was significantly increased relative to that in the 4 month Dp16 mouse. Total Tau levels failed to show significant differences for age or genotype (Figure S5l, n).

In summary, studies of m*App* gene expression in the Dp16 mouse brain demonstrated both similarities and differences with respect to those in the AD-DS and DS brain. While neither sex-dependent difference in CTF levels nor the increase of total Tau were recapitulated, consistent gene-dose linked changes in the levels of m*App* mRNA, fl-mAPP, mCTFs, and age-related increases in Aβ and Tau phosphorylation draw important parallels with AD-DS.

Effects of APP gene dose on neurodegeneration in Dp16 mice.: Loss of specific populations of vulnerable neurons is characteristic in AD and AD-DS, (reviewed [87]). Among vulnerable neuronal populations are those in layer II of the entorhinal cortex (EC) [88, 89], catecholaminergic neurons the locus coeruleus (LC) [90, 91], and cholinergic neurons in the basal forebrain magnocellular complex (BFCN) [92, 93]. To ask if the same populations are impacted in the Dp16 mouse, and to test for the necessity for increased m*App* gene dose for loss of neurons, we normalized the m*App* gene dose in Dp16 mice by producing Dp16 mice (*mApp* ++-) on the same strain background. We then examined Dp16, Dp16 (m*App* ++-), and 2N mice using unbiased stereology in the entorhinal cortex, locus coeruleus, and medial septum of the BFCN. By an average age of 16 months there were significant decreases in the number of neurons in Dp16 mice compared to 2N mice in BFCNs (p-value = 0.0474; Figure 4a panels, b) and LCNs (p-value = 0.0095; Figure 4d); however, there were no significant differences between 2N and Dp16 (*mApp* ++-) mice in either region. The analysis also revealed a significant difference in EC (p=0.014). Although post hoc analysis did not indicate which group(s) were different compared to 2N mice, the average number in Dp16 mice was lower than in either 2N or Dp16 (m*App*++-) mice. To examine p-Tau epitopes in Dp16 and 2N mice, we immunostained using a well-established antibody for IHC (PHF-1), which recognizes the phosphorylated sites at Ser396 and Ser404. At an average age of 16 months, accumulation of pTau-ir was readily seen in the Dp16 mouse cortex but not in Dp16 (m*App* ++-) mice; (Figure 4e panels) [94]. In Dp16 mice, quantitation of p-Tau-ir demonstrated an increase in pixel intensity (scale ranged from 0 = black to 255 = white) with respect to 2N mice, where the lower the number, the darker the pixel value, indicating greater immunoreactivity. ANOVA analysis revealed a significant difference between the groups (p-value = 0.0167; Figure 4f); however, *post hoc* analysis did not indicate which group(s) were significantly different compared to 2N mice. Nevertheless, the values for Dp16 (m*App*++-) approximated those of the 2N mouse. These findings are evidence that increased m*App* dose is necessary in Dp16 mice for the degeneration of

neurons vulnerable in AD-DS and for increased levels of an immunostaining marker of tau pathology.

To confirm the age-related degenerative nature of the reductions in neuron number we examined the same populations in the younger Dp16 mice. There were no significant differences at 4 months of age between the values in Dp16 normalized to 2N mice: Dp16 (0.9532 ± 0.0791) vs 2N (1.0 ± 0.3580) mice in ECNs (p-value = 0.8603); nor between the normalized numbers of LCNs: Dp16 (0.8658 ± 0.06901) vs 2N mice (1.0 ± 0.07367; p-value = 0.2544). Likewise, there was no significant difference (p-value = 0.9776) between Dp16 (1.005 ± 0.1172) and 2N (0.9998 ± 0.1012) mice in the number of BFCNs at 10 months of age. Similarly, PHF-tau immunoreactivity, using pixel intensity as a measure of densitometry, was not significantly different between Dp16, (176.5 ± 3.525) and 2N mice (186.4 ± 0.7686) in the entorhinal cortex at 4 months of age. These findings recapitulate age-related neurodegenerative phenotypes seen in AD-DS [89, 91, 95].

To document the expected reductions in *APP* products in the Dp16 (*mApp* ++-) mouse, we measured the levels of m*App* mRNA, fl-mAPP, mCTFs, and Aβ40 in all three genotypes (2N; Dp16 and Dp16 (*mApp* ++-)). We examined these measures in the cortex at age 4 months – i.e., before the onset of degeneration. Relative to 2N mice, in Dp16 mice the level of m*App* mRNA was increased about 2-fold and increases in the other *APP* products approximated those reported above. No significant differences were registered between 2N and Dp16 (m*App*++-) mice in any measure (Figure S5o–s). These data are evidence for gene-dose linked m*App* expression in the Dp16 model and confirm that increased levels of this gene are necessary for neurodegeneration. However, they do not identify a specific *APP* product as responsible.

Investigation of APP gene dose on microglial and astrocytes cells in Dp16 mice.: There is increasing recognition of a prominent role played by inflammation in the biology of AD the involvement of astrocytes and microglial cells [96, 97]. A recent report documented changes in microglial cells in young Dp16 mice, with changes detected as early as postnatal day 22 [98]. It reports in microglia cells a scavenging phenotype accompanied by a loss of dendritic spines in surrounding neurons. We assessed the status of activated microglial phenotypes, including ramifications of processes and size of microglial soma in the cortex of aged mice (16 months). We found that total process length, when normalized to the number of cells, was significantly decreased in Dp16 (p-value = 0.0252), but not in Dp16 (m*App*+ +-) (p-value = 0.2095) mice, as compared to 2N mice (Figure 4g). However, there was no significant difference in the size of microglia in Dp16 or Dp16 (m*App* ++-) mice compared to 2N mice (Figure 4h). These data are evidence for increased microglial activation in Dp16 versus 2N mice. Since process length, but not the microglia size, was a function of m*App* dose, microglial activation may be under the influence m*App* as well as other genes in Dp16 mice.

Astrocytes are involved in several processes in both the developing and mature brain [99], with astrogliosis present in AD-DS. To assess the possibility that astrocyte activation would characterize the young adult Dp16 brain, we again examined mice at age 4 months. Immunohistochemistry probing the entorhinal cortex show an elevated level of GFAP

immunoreactivity in both parenchyma tissue and near the vasculature of the Dp16 mouse brain (Figure 5a), but not in the medial septum (Figure 5b). Stereological analysis revealed a significant increase in the number of $GFAP^+$ astrocytes in Dp16 vs Dp16 (m*App*++-) mice in the entorhinal cortex: Dp16 = 1.39 x 10^5 cells/mm3; Dp16 (m*App*++-) = 0.63 x 10^5 cells/mm3); [(Dp16 versus 2N: p-value < 0.01; Dp16 versus Dp16 (m*App*++-): p-value <0.001)] (Figure 5a). However, stereological analysis revealed no significant increase medial septum in the number of $GFAP^+$ astrocytes in Dp16 vs Dp16 (m*App*++-) mice: Dp16= 1.11 x 10^5 cells/mm3; Dp16 (m*App*++-) = 1.03 x 10^5 cells/mm3); [(Dp16 versus 2N: p-value =0.90; Dp16 versus Dp16 (m*App*++-): p-value =0.92)] These data are evidence of an effect of the *App* gene dose on astrocyte activation in the entorhinal cortex, but not medial septum of Dp16 mice. Whether or not astrocytosis affects medial septum at later ages and what other regions are affected will require additional studies [100].

Investigation of APP gene dose on endosomes in Dp16 mice.: Dysregulation of early endosomes, with increased recruitment of Rab5 and enlargement, is an early feature of DS and is consistently present in AD-DS and AD [23, 24]. To explore a role for *APP* gene dose in this phenotype we asked if changes could be detected in young adult mice – i.e., at a time when increased m*App* expression was documented in Dp16 mice and demonstrated to be normalized in Dp16 (m*App*++-) mice. We examined the entorhinal cortex (Figure 5c–f) and medial septum (Figure 5g–j) of mice at age 4 months, comparing 2N mice to Dp16 and Dp16 (m*App*++-) mice. Tissue sections were stained with an antibody to Rab5 and random fields of the entorhinal cortex and medial septum were examined by fluorescent confocal microscopy and computer-aided morphometric analysis. Early endosomes with immunoreactivity for Rab5 in Dp16 were enlarged with an average size of 0.07 μm^2, compared to 0.06 μm^2 for both the Dp16 (m*App*++-) and 2N mice in the entorhinal cortex. Early endosomes with immunoreactivity for Rab5 in Dp16 were also enlarged in the medial septum (Figure 5h) with an average size of 0.08 μm^2, compared to 0.06 μm^2 for both the Dp16 (m*App*++-) and 2N mice. The enlargement of early endosomes in Dp16 mice in both the entorhinal cortex (Figure 5d) and medial septum (Figure 5h), though modest, was statistically significant, $p < 0.05$ with respect to both 2N and Dp16 (m*App*++-) mice. More revealing was the frequency distribution of individual Rab5 immunoreactive early endosomes in the entorhinal cortex (Figure 5d) and medial septum (Figure 5h). This showed that the observed increase in average puncta size was caused by an increase in the size of endosomes whose sizes were greater than 0.30 μm^2. Though constituting a minority of total endosomes, in these size classes the Dp16 mice had approximately twice as many puncta as for either 2N or Dp16 (m*App*++-) mice, which was statistically significant in the medial septum (Figure 5h; p-value < 0.05). In the entorhinal cortex the largest class of puncta (>0.50) was increased more than three-fold (Figure 5b). Whether or not endosomal enlargement is greater at later ages and registered in other brain regions is yet to be determined.

In summary, studies in the Dp16 mouse demonstrated the presence of degenerative hallmarks of AD-DS. In each case, the phenotype was normalized by reducing the m*App* gene dose. The findings are evidence that increased m*App* gene dose is necessary for several neurodegenerative phenotypes in this model of AD-DS.

Discussion

Overview:

Understanding AD pathogenesis is critical for defining treatments. Studies of causative mutations have identified possible mechanisms and greatly influenced clinical trials. Our findings addressed AD-DS, a condition that appears to offer an extraordinary additional opportunity to explore AD biology and treatment. Indeed, the increased risk for AD in the largest genetically defined population could prove singularly impactful. This assessment is supported by extensive evidence that neuropathological and clinical biomarkers of AD-DS largely recapitulate the findings in the non-DS population [1]. But we noted that clinical and pathological similarities must be viewed in the context of the different genetics created by trisomy of HSA21. We focused on the most compelling insight into AD in those with DS, that an extra copy of the gene for *APP* is necessary for a pathological AD diagnosis. The present study asked if increased *APP* dose was linked to increased gene expression in the brains of adults with DS and AD-DS. We compared the findings to ND controls and AD cases. We found that increased *APP* dose was correlated with increased levels of fl-hAPP and its hCTF and Aβ products, but that the pattern of increases was distinct from those in AD. Indeed, the AD-DS brain showed higher levels of detergent-soluble Aβ and sex-dependent differences for hCTFs and fl-APP processing enzymes in AD-DS females. These findings argued against attributing to any APP product a singular role in pathogenesis. Moreover, partial trisomy and mosaic DS cases identified changes in *APP* products inconsistent with the view that *APP* gene-dose alone regulates their levels. Taken together, the evidence suggests that the products of genes on HSA21, as well as other chromosomes, impact the levels of APP products. Further differentiating AD-DS from AD were greater increases in the levels of pT212 and total tau. To support the ability to incisively explore AD-DS pathogenesis we asked if the Dp16 mouse models of DS captured the changes detected in DS and AD-DS (Table 3). Increased m*App* dose was routinely correlated with proportional increases in fl-mAPP and mCTFs from young to old age. The single exception was the small increase in mCTFs relative to fl-mAPP in the hippocampus of old mice. The same proportionality was seen for Aβ levels, but with a relative increase in both Aβ40 and Aβ42 in the oldest mice. The Dp16 model also recapitulated the increase in pT212. Most important, increased m*App* dose was necessary for the loss of neurons known to be vulnerable in AD and AD-DS as well as other markers of AD pathogenesis. Taken together, the findings confirm the importance of increased *APP* dose for AD in DS, give new insights into the mechanisms that contribute, and create a roadmap for future studies to define how increased APP acts to cause AD-DS.

Updating the *APP* dose hypothesis for AD-DS:

The simplest formulation of the *APP* dose hypothesis is that an extra copy of the gene acts via increases in each of the gene's products, one or more of which are responsible for age-related emergence of AD pathology and dementia. Increased *APP* dose was reflected in increased product levels in DS and AD-DS. These data are important because although it has been assumed that an increase in *APP* would result in increased *APP* products, the direct demonstration has been lacking in those who based on age are at increased risk or who have been diagnosed with AD-DS. Consistent with earlier reports [32, 34–48], we

confirmed that relative to ND controls and AD increased *APP* gene dose in DS was linked to increased levels of fl-hAPP. This increase approximated gene dose. We also found increases in hCTFs in males in proportion to fl-hAPP levels. In females, the levels of CTFs were greater than expected. Our findings differ from an earlier study reporting no increase in hCTFs versus fl-hAPP in DS cases over age 40, but males and females were not separated in that study [37]. Remarkably, in both males and females with AD-DS, the levels of Aβ42 and 40 significantly exceeded levels expected based on fl-hAPP and also exceeded those in AD. Increased detergent soluble Aβ species in DS and AD-DS complement earlier findings for increased amyloid plaque size in DS versus AD [101, 102] and draw a strong parallel with an earlier study demonstrating marked increases relative to controls in formic acid-soluble Aβ [37]. Our findings thus inform the hypothesis by confirming increases in several *APP* products. They update the hypothesis by indicating that changes in product levels are not a simple function of gene dose and argue against attributing to a specific product a singular role in pathogenesis. Thus, in contrast to the amyloid hypothesis of AD, and despite many clinical and pathological parallels with AD, the pathogenesis of AD-DS cannot be solely attributed at present to increased levels of Aβ species. It will be essential to define the specific *APP* product(s) responsible for AD-DS. The exciting possibility exists that these studies may speak to additional *APP* products also active in AD. Two additional interesting possibilities address the increases in APP products in AD-DS. The first is that increased levels of such products may exceed clearance mechanisms, further exacerbating the increases. The second is that increased levels of Aβ might compete with CTFs for processing by γ-secretase, thus creating a feedback inhibitory loop that could increase the levels of both. Further studies will be needed to address these possibilities.

We noted that hCTFs levels differed between males and females with AD-DS; the increase in females exceeded those in males even though they demonstrated approximately the same increase in fl-hAPP. Increased hCTFs were also present in DS females not diagnosed with AD-DS. We have not defined the source(s) of this sex-related difference. However, we also noted significantly increased levels of fl-hAPP processing enzymes of the BACE pathway (BACE1 (mature) and BACE2) in AD-DS females versus ND females; increases relative to AD-DS males and ND males were also present. It is possible that increased BACE activity resulted in increased production of hCTFs in AD-DS females relative to these other cases. But two findings in AD-DS females refute this suggestion. The first is that while the absence of a corresponding increase in mature ADAM10 in AD-DS females would predict an increase in the ratio of β-hCTFs to α-hCTFs in AD-DS females, but this was not observed. Consistent with Nistor *et al.*, [37], we found no difference in the relative levels of α-hCTFs and β-hCTFs in AD-DS cases versus ND. These authors detected an age-related increase in DS in β-hCTFs and the ratio of β-hCTFs to α-hCTFs. However, in elderly controls (>age 40 years) the values in controls for α-hCTFs/total hAPP, β-hCTFs/total hAPP, and the ratio of β-hCTFs to α-hCTFs overlapped those for DS, consistent with our results. A second finding that casts doubt on a role for increased BACE pathway activity in increasing hCTFs in AD-DS females is that these cases also showed increases in Nicastrin and PEN2. This might lead to lower, not higher levels of hCTFs in AD-DS females. Adding to the evidence that the levels of *APP* products are under the control of other genetic and possibly age-related factors are the findings in the PT-DS male and mosaic female. Here we found increased

hCTFs that could not be accounted for based on *APP* dose or level of fl-hAPP. Moreover, both showed an increase in the ratio α-hCTFs to β-hCTFs. Accordingly, to explicate the role that increased *APP* dose has for AD-DS future studies could explore how other genes and regulatory sequences on HSA21 contribute.

Sex-based differences in AD-DS:

The differences between AD-DS females and males adds to a growing literature for sex-dependent differences in AD. One is for the increased prevalence of AD, with more females developing AD compared to males, even after correcting for confounding factors (reviewed [103]). However, the significance of sex-differences in AD-DS is yet to be firmly established at the clinical level. A recent cross-sectional analysis of California Medicare recipients showed no sex-dependent differences in the number of people with DS diagnosed with dementia [104]. Although some studies failed to show sex-dependent differences in life expectancy in the DS population [105], others reported a shorter survival for men diagnosed with dementia as compared to women [26]. It has been suggested that women are diagnosed at an earlier age or that symptoms of AD are more likely to be missed in men, resulting in an apparent shorter survival time after diagnosis [26]. Additionally, studies have shown a correlation between early entry into menopause and onset of dementia in women with DS; onset of menopause is typically in the early ‘40s and ‘50s [106–109]. Since low estrogen and progesterone levels in females have been associated with a higher risk of AD (reviewed in [110, 111]), one possible source for sex differences could be hormonal effects on the processing and degradation of fl-hAPP and its products. We note that BACE1 expression is under the control of both an estrogen response element and a progesterone response element [112] pointing to possible regulation by either or both hormones. Neprilysin (NEP), the primary enzyme responsible for Aβ clearance, is also modulated by hormones [113] and glucocorticoids [114]. Whether or not NEP or other A degrading enzymes have a role in explaining the sex differences in AD-DS merits further study. Our finding of significant differences in AD-DS females as compared to males provides additional motivation for exploring sex-related differences in the processing of fl-APP and its products to further inform the *APP* gene dose hypothesis.

Observations in the Dp16 model inform the hypothesis:

We examined the Dp16 mouse to ask if neurodegenerative features of AD-DS could be replicated, whether increased m*App* dose was necessary to demonstrate them, and if so to ask how findings in the mouse could be used to further inform the *APP* gene dose hypothesis in AD-DS. The discovery that reducing m*App* dose in the Dp16 mouse prevented loss of vulnerable neurons and other AD-relevant markers established this model as potentially useful, in so doing significantly extending our earlier studies [115, 116]. Perhaps most salient was that the changes in Dp16 mice are produced in the setting of DS-relevant proportional increases in fl-mAPP and mCTFs and in the absence of levels of Aβ that attend amyloid plaque formation. These findings constrain the *APP* dose hypothesis by arguing that plaques are not a necessary contributor to neurodegeneration. However, they do not argue against a role for Aβ or amyloid plaques. We did find subtle age-related increases in Aβ40 and Aβ42 that may have contributed. Moreover, in AD the presence of neuritic dystrophy in and near plaques suggests that plaques do exert toxicity [117]. Our findings argue that

whatever role(s) the plaque has, it is not essential for the death of neurons, for increased tau pathology, or activation of astrocytes and microglial cells. The argument against amyloid plaques as the sole or even necessary contributor to pathological manifestations in AD is increasingly accepted; the reconsideration of the amyloid hypothesis now points to a role for toxic oligomeric complexes of Aβ ([118]; see [78] for review), a species that could have been present in the Aβ samples examined herein.

Future directions in hypothesis testing:

How might an increase in *APP* dose act to induce AD pathogenesis in those with DS? Our findings in both human and the mouse model inform this question. First, a role for fl-hAPP has not been ruled out. Studies of fl-APP should be carried out in systems that express this product at levels approximating gene dose in DS. Marked increases in *APP* gene expression may compromise the ability to evaluate DS-relevant mechanisms. Studies of synthesis, trafficking, and clearance of fl-APP should be under conditions and in models that allow for sensitive measurement of these parameters. Second, studies of the same type should address a role for CTFs, again examining this species under conditions proportional to increased *APP* dose in DS. This recommendation does not obviate further evaluation of the impact of sex on hCTF levels. Indeed, it will be important to further explore how sex impacts this measure and into sex effects on fl-APP processing enzymes. However, since other measures of *APP* products in AD-DS failed to differentiate males and females the increase in hCTFs may not have been a necessary contributor. Essential to the evaluation of hCTFs is their distribution within the cell and the levels therein, as will be discussed below. Finally, understanding the production and clearance of Aβ species is essential for understanding the impact of *APP* dose. The findings in the DS and AD-DS brain suggest that increased *APP* dose may impact both the production and clearance of Aβ peptides, especially Aβ42 and 40. This observation motivates studies to explore the anatomical compartments in which the increases are registered. Localized increases that distinguish AD from AD-DS could result in differential involvement of cellular compartments and potentially the creation of more toxic oligomeric Aβ species, speculations that can now be evaluated.

Testing the hypothesis requires addressing several questions. The first and most important is which *APP* product plays a role. Our studies in human brains and the Dp16 mouse do not allow a conclusion, nor do they rule out the participation of more than one APP species. The second question is where and how do the implicated product(s) act. With what proteins does it interact, in what cellular compartment, and through what process(es)? A third question is how the genetic environment created by DS informs the interactions and processes thus identified. Our studies of gene expression in the Dp16 mouse give evidence of changes in expression not only of triplicated genes but of others whose products contribute to AD. Studies in the DS brain will be needed to further address possible genetic links, including the participation of genes on HSA21 that may modify pathogenesis. A prominent HSA21 candidate is DYRK1A whose kinase activity impacts many substrates [13]. Its contribution to AD pathogenesis may be through effects on tau splicing and phosphorylation of tau as well as fl-APP [119]. DYRK1A targets tau at T212 [13, 120], thus priming tau for phosphorylation by GSK3-β [120]. Increased pT212 levels in AD-DS in our studies raise the possibility that increased *DYRKA1* gene dose plays a role. This suggestion is supported

by increased pT212 also in the Dp16 model. The increase in pT212 in both AD-DS and the aged Dp16 mouse suggests that age interacts with the DS genetic environment to manifest AD-relevant phenotypes. Accordingly, it will be important to consider age as an independent contributor to pathogenesis in AD-DS. Finally, given the evidence that non-neuronal cells, as well as neurons, participate in the biology of AD [97], and our findings for astrocytes and microglia in the Dp16 mouse, future studies should explore how increased *APP* dose impacts each of the cell types in the CNS.

Benefits and limitations of model systems for hypothesis testing:

The Dp16 mouse provided a testing environment for the hypothesis. While some features in AD-DS were recapitulated, neither the marked increases in Aβ species nor sex-related differences were reproduced. The failure of Aβ to accumulate in mice expressing wild-type mouse APP, even at levels greater than present in humans with DS, is a function of structural differences in the mouse and human proteins. Different amino acids at three positions within the Aβ sequence of the human protein increase considerably BACE processing, yielding higher levels of β-CTFs and their Aβ peptide products [121]. In an attempt to fully recapitulate the change in the DS brain, it will be necessary to 'humanize' the Aβ region in the endogenous mouse gene in the Dp16 mouse. Whether or not h*APP* expression at levels 150% of those in 2N mice will significantly increase Aβ accumulation is unknown. Earlier studies in which wild-type h*APP* was expressed at levels approximately equal to and greater than the endogenous mouse gene contained readily measurable levels of human Aβ species, including Aβ42, but did not contain plaques [122]. Remarkably, however, even in the absence of plaques, wild-type h*APP* expressing mice showed reduced synaptophysin-immunoreactive presynaptic terminals, arguing for toxic manifestations directed at synapse number. The humanized Dp16 mouse may show similar changes. Alternatively, in the context of an increase in copy number of genes relevant to AD-DS the changes may be more dramatic, including plaque formation. If so, the participation of other genes can be addressed. Studies in mouse models in which the humanized *APP* is expressed at a range of levels may also inform a level for increases in Aβ that changes clearance and accumulation of this peptide beyond what is seen in AD. Furthermore, these studies will allow an examination of the impact on the pathogenesis of a more complete set of *APP* products through mutations that modify cleavage via α-secretase, β-secretase, and γ-secretase. Particularly useful may be a new mouse model of DS in which a copy of HSA21 has been added to the mouse genome [123]. TcMAC21 contains 93% of the expressed HSA21q protein-coding genes and recapitulates brain phenotypes characteristic of DS, albeit not amyloid plaques. Studies using this model, promise additional insights into the contribution of the genes on HSA21. Critical to all the studies just outlined will be the extent to which APP, and possibly other HSA21 gene products, replicates the molecular and cellular changes responsible for neurodegeneration in AD-DS.

Another model system to be examined is that provided by the human brain itself. Single-cell RNA seq studies are providing novel insights into the cells and molecular programs impacted by AD [124]. Studies of this type in AD-DS are likely to prove highly informative. The most obvious limitation is that one is capturing the 'snapshot' of changes present at the postmortem exam, as did our studies. Nevertheless, valuable insights may be forthcoming

that will prove essential for informing pathogenesis. These data will be more readily interpreted if complemented by studies in the brains of those with DS that die at earlier ages.

Ideally, a model of DS in which *APP* gene dose is increased in non-human primates would be employed. Perhaps the most significant limitation in studies in the mouse is that the rodent brain differs considerably from that of the human; differences in size, regional anatomy, and complexity are all appreciated. Accordingly, the cognitive and behavioral repertoires of humans are far greater than those of the mouse. In particular, the rich social and cognitive life of humans cannot be effectively modeled in the mouse. For these reasons, attention has increasingly focused on the development of non-human primate (NHP) models for human brain disorders, a context in which a more human-like genome is expressed, and in which *APP* gene dose might be examined more incisively. Though not currently available, such a model could increase the ability to examine age-related changes for the impact of increased *APP* dose in a more human-like context [125]. An added benefit would be the ability to explore human-like behaviors [126].

Studies of the *APP* dose hypothesis stand to benefit considerably by the ability to use fibroblasts and other tissues to generate neurons and other CNS cell types via iPSC or direct induction. Indeed, studies of this type promise the ability in vitro to evaluate cellular mechanisms under the influence of human genes with great precision. The development of 3-D cultures [127] as well as organoids [128] can be used to examine the environment created by increased *APP* dose. Studies using organoids have been used to study DS [129]. Interestingly, a recent report examining DS iPSC-derived neurons and cerebroids found that reducing *BACE2* copy number resulted in increased AD-relevant pathology, suggesting that trisomy for *BACE2* in DS acts to suppress AD through proteolytic events targeting processing of Aβ [130]. Limitations exist for use of these methods. Aging serves as a major concern in that iPSC-derived cultures recapitulate early stages in neuronal development; this may be less significant for the *APP* dose hypothesis given that even young neurons are impacted by increased *APP* dose, at least as reflected in endosomal pathology [24]. A second concern is for lack of vascularization, which may impact cell viability and cellular differentiation; the blood-brain barrier constitutes an important element in brain function and may be impacted by Aβ deposition leading to cerebrovascular amyloid in the DS brain [131]. Attempts to overcome this limitation are being explored [132]. Another is the need to create cultures with all the relevant CNS cell types, including oligodendroglia and microglial cells. Advances are being made to address this need as well as to increase the production of uniform cultures. In summary, while limitations are recognized, much progress is being made to address the use of human models of AD (for reviews see [128]). Importantly, even relatively simple models may serve to explore questions raised by the *APP* dose hypothesis.

Speculations on a mechanism by which increased *APP* dose acts in DS to cause AD-DS:

Though there is much to learn, based in part on our data in AD-DS and the mouse it is possible to offer speculation as to how *APP* gene dose leads to AD. We argue that dysregulation of the endosomal/lysosomal pathway could account for many disease manifestations, including synaptic dysfunction and loss. This speculation is supported by

the work of many laboratories over the years, most prominently the work of Ralph Nixon and colleagues, as has recently been summarized [133–136]. Key observations include: 1) fl-APP is processed to both hCTFs and Aβ within the endosomal compartment [137]; 2) enlargement of early endosomes, with increased activation of the small GTPase Rab5, is observed in sporadic AD, AD due to *APP* duplication and mutations, as well as AD-DS; 3) indeed, early endosome enlargement is the earliest pathology demonstrated in sporadic AD and is already present prenatally in DS [23, 24]; and 4) changes in early endosomes are later correlated with changes in other compartments of the endosomal/lysosomal as well as in autophagosomes in AD [133, 136].

Relative to the *APP* gene dose hypothesis, two important questions arise. Which APP product(s) are responsible for endosomal changes, and how do endosomal changes induce neurodegeneration. Regarding the former, the evidence is compelling that β-CTFs are important in endosomal dysfunction and pathogenesis [135, 138–140]. Indeed, studies in animal models of DS, rodent neuronal cultures in which APP products are expressed in excess, and iPSC-derived human neurons carrying familial AD mutations combine to support a role for β-CTFs [135, 138, 139, 141–143]. It is not clear how to explain increased endosome size in sporadic AD wherein *APP* is not overexpressed, but evidence for increased β-CTFs has been reported [139]. The mechanism by which increased β-CTF results in increased activation of Rab5 and endosome enlargement is through recruitment of APPL1 (adaptor protein containing pleckstrin homology domain, phosphotyrosine binding domain, and leucine zipper motif), a scaffolding protein that anchors the CTF to Rab5 [139]. As indicated, we found increases relative to actin in both α-hCTFs and β-hCTFs in both AD-DS males and females, but no increase in the ratio of these species in comparison with NDs. Efforts to examine further the levels and cellular compartments containing CTFs will benefit from a larger number of cases, use of advanced tissue imaging methods, high-resolution gel systems, and the use of proteomic analyses. It is possible [134] that other APP products may contribute to endosomal enlargement and dysfunction [138]. Since γ-secretase serves to process both CTFs and Aβ, an intriguing possibility is that Aβ present at high concentrations within the endosome inhibits the processing of CTFs. Studies to test this idea and to more fully examine the impact of the fl-hAPP and Aβ products are needed to further inform which APP products act to dysregulate endosomes.

How, would a change in the endosomal compartment act to cause neurodegeneration? Beyond the important role that the endosomal compartment plays in protein and lipid metabolism and degradation, the literature points to a role for endosomes, including the early endosome, in the trafficking of signaling receptors within the neuron. The signaling endosome hypothesis points to the endosomal compartment as an essential support for long-distance communication of the signals of neurotrophic factors [134]. Enlarged endosomes less effectively convey neurotrophic signals in vitro and in vivo [115] and there is a correlation between neurodegeneration and *APP* gene dose-mediated increases in endosomal dysregulation [115]. A recent report showed that reducing in vitro the translation of m*App* mRNA in the Ts65Dn mouse reduced fl-mAPP and mCTFs, reversed Rab5 hyperactivation and early endosome enlargement, and restored retrograde transport of neurotrophin signaling. In vivo, reducing translation of the mRNA for m*App* also reduced fl-APP and mCTFs, restored normal levels of Rab5 activity, reduced p-tau, and

reversed deficits in TrkB (tropomyosin receptor kinase B) activation and in the Akt (protein kinase B [PKB]), ERK (extracellular signal-regulated kinase), and CREB (cAMP response element-binding protein) signaling pathways [144]. Nixon and colleagues have powerfully complemented and extended these findings by showing that forced increases in the activity of Rab5 resulted in endosomal enlargement, induced changes in both long-term potentiation and long-term depression in the hippocampus, reduced AKT signaling, reduced surface levels of glutamate receptors, increased p-tau, and caused degeneration of BFCNs [135]. Taken together the data are compelling that dysfunction of the endosomal system, initiated through increased activation of Rab5, powerfully induces AD-relevant changes. It remains to be defined when increased *APP* dose results in changes in endosome signaling, how they progress and whether they are necessary for the loss of synapses that characterizes AD and AD-DS. While increased *APP* dose may well have effects beyond changes in endosomes and the endosomal/lysosomal system, the two phenomena are linked and deserve careful study, especially given the evidence that neurotrophic signaling contributes to the function of mature neurons and their synapses [145]. Quite possibly, the age-related changes characteristic of AD-DS may reflect the cumulative result of many years of subtle reductions in neurotrophin signaling.

Treating to counter the effects of increased *APP* gene dose in AD-DS:

The discovery that *APP* gene dose plays a necessary role in AD-DS can focus therapeutic attempts to target *APP* gene expression. Thus, beyond studies to explore the mechanism by which *APP* gene dose leads to AD, the use of models of DS in which increased *APP* dose is linked to degenerative phenotypes will facilitate studies of potential treatments. Our findings make clear that the Dp16 mouse is well suited to such studies. The other animal model systems referenced above are also appropriate, as are those examining human neurons. Interventions would examine both target engagement – i.e., reduced levels of the products of APP – as well as normalization of the events downstream from increased *APP* dose. Thus, examining treatments targeting *APP* dose should include observations of changes in the levels of activity and trafficking of fl-App-interacting proteins, endosome structure, and signaling, synapse number, and activity, as well as circuit function and cognition. Measured improvements in cellular and brain functions linked to neurodegeneration will be of greatest interest.

Having stressed the need for deciphering which APP products induce degenerative phenotypes and the mechanism(s) by which they act, even without a full accounting of pathogenesis the evidence that increased *APP* dose induces AD-DS is sufficient to motivate interventions to reduce their levels. In DS, the goal would be to reduce to normal the levels of *APP* mRNA and its protein products. Building on experience in other degenerative disorders [146, 147], antisense oligonucleotides specifically directed against *APP* mRNA may serve as an RNA-targeting treatment to reduce *APP* mRNA levels. Studies in mouse models of DS [148] and AD mouse models have been reported [149–151]. The use of ASOs is frustrated by an inability to deliver them to the brain via systemic injection. Thus, intrathecal delivery of ASOs may be required; this mode of delivery would require repeated administration but has the advantages of high selectivity for *APP* mRNA. Moreover, targeting h*APP* mRNA will enable dose modifications using measures of Aβ levels in

CSF and possibly plasma. siRNAs against *APP* represent another RNA-based approach [152]. Importantly, recent studies encourage the view that modified reagents may enable CNS penetration of systemically delivery of RNA-based treatments [153]. Alternatively, small molecules that interfere with the translation of *APP* mRNA could prove effective. Posiphen is one such molecule. As reported above, in recent studies we found that Posiphen normalized fl-mAPP and mCTFs and restored endosomal function [144]. Aβ42 and Aβ40 are additional treatment targets. In one approach, trials of BACE inhibitors were conducted. They were stopped for futility and/or toxicity; for several treatments worsened cognitive decline was detected. Thus, at present no clear role has emerged for this class of reagents [154]. Unfortunately, but possibly not surprising given data for the links between β-CTFs and endosomal dysfunction, clinical trials using inhibitors of the γ-secretase enzyme (i.e., GSIs) failed to improve outcomes and demonstrated untoward side effects including worsening of cognition [155–158]. More encouraging are findings in recent preclinical findings of small molecule γ-secretase modulators (GSMs), which appear to act by enhancing processivity of the exopeptidase activity of the enzyme [159]. Chronically administered to PSAPP mice, the GSMs reduced plasma and brain levels of Aβ42 and Aβ40, prevented plaque deposition in young mice, and retarded plaque growth in older mice [160].

Immune approaches represent another potentially useful modality and are the focus of several ongoing trials [154]. A vaccine directed at Aβ was tested in the Ts65Dn mouse model of DS. Vaccination was safe and resulted in excellent titers with a modest, statistically insignificant reduction in brain Aβ levels relative to vehicle-treated mice. Vaccinated mice showed improvement in memory deficits and reduced atrophy of BFCNs [161]. These data, the first to show that an anti-Aβ immunotherapeutic approach may act to target Aβ-related pathology in a mouse model of DS, inspired a Phase 1b study in adults with DS. The trial was recently completed, and results are expected to be reported soon. The several recent and ongoing trials of antibodies to Aβ in sporadic AD [162, 163] are yet to give evidence of convincing clinical benefit. They do however point to the rather consistent ability to remove amyloid plaques and modestly reduce the progression of cognitive loss. Amyloid-related imaging abnormalities (ARIAs) induced by antibody engagement of plaques is a recognized adverse event and a continuing concern. Increased plaque load and significant cerebrovascular amyloid and vascular pathology in DS [131] cautions the need for attention to this safety signal in DS.

Studies of *APP* dose effects in DS are expected to yield new insights into possible treatment targets. The evidence showing a role for increased β-CTFs in inducing increased activation of Rab5 raises the possibility that Rab5 activation may also serve as a target. Though how best to target increased Rab activity is yet to be defined, one approach would be the delivery of ASOs specific to one or more of the Rab5 isoforms. Reducing Rab5-GTP levels to normal is rational and deserving of further study.

Conclusion:

Increased *APP* gene dose is necessary for AD in those with DS. Herein we tested the hypothesis that *APP* gene dose results in increased levels of its products. We confirmed

increases in the brain levels of fl-hAPP and its products in DS and AD-DS. The effect of increased *APP* dose was registered at the level of fl-APP, CTFs, and Aβ peptides. Increases in detergent soluble Aβ42 and Aβ40 beyond those expected based on fl-hAPP levels were noted in AD-DS males and females; these increases exceeded not only those in ND controls but also males and females with sporadic AD. A sex effect was documented for hCTF increases greater than fl-hAPP in AD-Ds females and was correlated with increases in proteins that contribute to BACE and γ-secretase processing of fl-hAPP. Extending our hypothesis testing to the Dp16 mouse model of DS, we found dose-related changes in fl-mAPP and its products. Drawing an important parallel with AD-DS, increased m*App* dose was necessary for neurodegenerative phenotypes, affirming a role for *APP* dose and pointing to the utility of this model for future studies.

Our findings point to the importance and utility of deciphering critical gaps for elucidating the *APP* gene dose hypothesis. Which *APP* product(s) contribute, the mechanism(s) of action induced, the timing of their induction, and how to counter them are each critical for ultimately understanding and treating to prevent the impact of increased *APP* dose. Especially important will be studies that examine the steps that link increased *APP* dose to synaptic dysfunction and degeneration, including those to comprehensively examine a role for disruption of endosomal signaling and trafficking. Past experimental barriers to addressing these gaps are mitigated by powerful new model platforms, both rodent and human, and through technological advances that increase the ability to interrogate individual cell populations and their products in the brain. Even now, existing and new treatment modalities targeting increased *APP* products can be considered for blocking pathogenesis of AD in DS.

Supplementary Material

Refer to Web version on PubMed Central for supplementary material.

Acknowledgments

We are grateful to Elsa Molina, Ph.D., Director of the UC San Diego Stem Cell Genomics Core for the technical assistance during NanoString experiments. This work was made possible in part by the CIRM Major Facilities grant (FA1-00607) to the Sanford Consortium for Regenerative Medicine; NIH R01AG055523 and R01AG061151 (WM); Ono Pharma Foundation: UCSD 2019-0742 (WM); and DH Chen Foundation: R-86U55A (WM); NIH/NIA U19AG068054, P30AG066519 (EH) and NIH R01NS066072 (WM and YEY).. We thank the many participants and their family members for participating in the brain donation programs that made our studies possible. We are grateful to the Banner Sun Health Research Institute Brain and Body Donation Program of Sun City, Arizona for the provision of human biological materials (or specific description, e.g., brain tissue, cerebrospinal fluid). The Brain and Body Donation Program has been supported by the National Institute of Neurological Disorders and Stroke (U24 NS072026 National Brain and Tissue Resource for Parkinson's Disease and Related Disorders), the National Institute on Aging (P30 AG19610 Arizona Alzheimer's Disease Core Center), the Arizona Department of Health Services (contract 211002, Arizona Alzheimer's Research Center), the Arizona Biomedical Research Commission (contracts 4001, 0011, 05-901 and 1001 to the Arizona Parkinson's Disease Consortium) and the Michael J. Fox Foundation for Parkinson's Research. The authors have no relevant financial or non-financial interests to disclose.

Declaration of Interests

Funding directly supporting this study was provided by the CIRM Major Facilities grant 9 (FA1-00607) to the Sanford Consortium for Regenerative Medicine; NIH R01AG055523 and R01AG061151 10 (WM); DH Chen Foundation: R-86U55A (WM); NIH/NIA U19AG068054, P30AG066519 (EH), NIH R01NS066072 (WM and YEY). The following entities provided support in the form of tissues and/or biological specimens. There was no

monetary support provided. Banner Sun Health Research Institute Brain and Body Donation Program of Sun City, Arizona for the provision of human biological materials (brain tissue). The Brain and Body Donation Program has been supported by the National Institute of Neurological Disorders and Stroke (U24 NS072026 National Brain and Tissue Resource for Parkinson's Disease and Related Disorders) the National Institute on Aging (P30 AG19610 Arizona Alzheimer's Disease Core Center), the Arizona Department of Health Services (contract 211002, Arizona Alzheimer's Research Center), the Arizona Biomedical Research Commission (contracts 4001, 0011, 05-901 and 1001 to the Arizona Parkinson's Disease Consortium) Michael J. Fox Foundation for Parkinson's Research (TB). In the past 36 months funding was provided by NIH (NIA AND NINDS) to WM; Ono Pharma Foundation to WM; Cure Alzheimer Fund to WM; DH Chen Foundation to WM; AC Immune to WM; Larry L Hillblom Foundation to WM; Alzheimer Association to WM. Avid Radiopharmaceuticals, National Institutes of Health, Michael J Fox Foundation, and Arizona Department of Health Services to UCSD for TB. U19AG068054 and UCI P30AG066519 were awarded to UCI for EH. All other relationships/activities/interests: Consulting fees were paid to WM from Samumed and AC Immune; to AS from Darmiyan and Sybaretic; to TB from Vivid Genomics. Honoraria were paid to WM for NIH study section and TB from Roche Diagnostics. Travel reimbursements were made to WM from AC Immune for SfN and to MS from UCSD for SfN 2018. WM provided expert testimony for the law firm of Koren-Tillery. Patent interests are held by UCSD on behalf of WM for Gamma-secretase Modulators, and AS for virtual reality for the diagnosis of Alzheimer's disease. WM participated on a safety monitoring board for Pfizer. WM holds leadership and/or fiduciary roles in 21 Research Society (no payments); Society for Neuroscience (reimbursement for travel); Alzheimer San Diego (no payments); American Neurological Association (no payments; NIH (COBRE Grant to the University of Nebraska) (no payments); The Bluefield Project to Cure Frontotemporal Dementia. TB is on the scientific advisory board for Vivid Genomics (no payments). YEY is on the executive board for T21RS (no payments). WM holds stock or stock options in Annovis Bio; Alzheon; Curasen; Cortexyme; and Promis. TB holds stock options in Vivid Genomics. Annovis Bio has provided a gift to the WM lab and provided test compound.

References

[1]. Snyder HM, Bain LJ, Brickman AM, Carrillo MC, Esbensen AJ, Espinosa JM, et al. Further understanding the connection between Alzheimer's disease and Down syndrome. Alzheimers Dement. 2020;16:1065–77. [PubMed: 32544310]

[2]. Stoll C, Alembik Y, Dott B, Roth MP. Epidemiology of Down syndrome in 118,265 consecutive births. American journal of medical genetics Supplement. 1990;7:79–83. [PubMed: 2149980]

[3]. de Graaf G, Buckley F, Skotko BG. Estimation of the number of people with Down syndrome in the United States. Genet Med. 2017;19:439–47. [PubMed: 27608174]

[4]. Presson AP, Partyka G, Jensen KM, Devine OJ, Rasmussen SA, McCabe LL, et al. Current estimate of Down Syndrome population prevalence in the United States. The Journal of pediatrics. 2013;163:1163–8. [PubMed: 23885965]

[5]. Antonarakis SE, Skotko BG, Rafii MS, Strydom A, Pape SE, Bianchi DW, et al. Down syndrome. Nature reviews Disease primers. 2020;6:9.

[6]. Hassold T, Hunt P. To err (meiotically) is human: the genesis of human aneuploidy. Nat Rev Genet. 2001;2:280–91. [PubMed: 11283700]

[7]. Antonarakis SE, Avramopoulos D, Blouin JL, Talbot CC Jr., Schinzel AA. Mitotic errors in somatic cells cause trisomy 21 in about 4.5% of cases and are not associated with advanced maternal age. Nat Genet. 1993;3:146–50. [PubMed: 8499948]

[8]. Antonarakis SE. Parental origin of the extra chromosome in trisomy 21 as indicated by analysis of DNA polymorphisms. Down Syndrome Collaborative Group. N Engl J Med. 1991;324:872–6. [PubMed: 1825697]

[9]. Zigman WB. Atypical aging in Down syndrome. Dev Disabil Res Rev. 2013;18:51–67. [PubMed: 23949829]

[10]. Ballard C, Mobley W, Hardy J, Williams G, Corbett A. Dementia in Down's syndrome. The Lancet Neurology. 2016;15:622–36. [PubMed: 27302127]

[11]. Lott IT, Head E. Dementia in Down syndrome: unique insights for Alzheimer disease research. Nat Rev Neurol. 2019;15:135–47. [PubMed: 30733618]

[12]. Antonarakis SE, Lyle R, Chrast R, Scott HS. Differential gene expression studies to explore the molecular pathophysiology of Down syndrome. Brain Res Brain Res Rev. 2001;36:265–74. [PubMed: 11690624]

[13]. Duchon A, Herault Y. DYRK1A, a Dosage-Sensitive Gene Involved in Neurodevelopmental Disorders, Is a Target for Drug Development in Down Syndrome. Frontiers in behavioral neuroscience. 2016;10:104. [PubMed: 27375444]

[14]. Kleschevnikov AM, Yu J, Kim J, Lysenko LV, Zeng Z, Yu YE, et al. Evidence that increased Kcnj6 gene dose is necessary for deficits in behavior and dentate gyrus synaptic plasticity in the Ts65Dn mouse model of Down syndrome. Neurobiol Dis. 2017;103:1–10. [PubMed: 28342823]

[15]. Lockstone HE, Harris LW, Swatton JE, Wayland MT, Holland AJ, Bahn S. Gene expression profiling in the adult Down syndrome brain. Genomics. 2007;90:647–60. [PubMed: 17950572]

[16]. Olmos-Serrano JL, Kang HJ, Tyler WA, Silbereis JC, Cheng F, Zhu Y, et al. Down Syndrome Developmental Brain Transcriptome Reveals Defective Oligodendrocyte Differentiation and Myelination. Neuron. 2016;89:1208–22. [PubMed: 26924435]

[17]. Do C, Xing Z, Yu YE, Tycko B. Trans-acting epigenetic effects of chromosomal aneuploidies: lessons from Down syndrome and mouse models. Epigenomics. 2017;9:189–207. [PubMed: 27911079]

[18]. Capone GT, Chicoine B, Bulova P, Stephens M, Hart S, Crissman B, et al. Co-occurring medical conditions in adults with Down syndrome: A systematic review toward the development of health care guidelines. Am J Med Genet A. 2018;176:116–33. [PubMed: 29130597]

[19]. Soria Lopez JA, Gonzalez HM, Leger GC. Alzheimer's disease. Handb Clin Neurol. 2019;167:231–55. [PubMed: 31753135]

[20]. Wisniewski KE, Wisniewski HM, Wen GY. Occurrence of neuropathological changes and dementia of Alzheimer's disease in Down's syndrome. Ann Neurol. 1985;17:278–82. [PubMed: 3158266]

[21]. Head E, Lott IT, Wilcock DM, Lemere CA. Aging in Down Syndrome and the Development of Alzheimer's Disease Neuropathology. Curr Alzheimer Res. 2016;13:18–29. [PubMed: 26651341]

[22]. Xue QS, Streit WJ. Microglial pathology in Down syndrome. Acta Neuropathol. 2011;122:455–66. [PubMed: 21847625]

[23]. Cataldo AM, Petanceska S, Terio NB, Peterhoff CM, Durham R, Mercken M, et al. Abeta localization in abnormal endosomes: association with earliest Abeta elevations in AD and Down syndrome. Neurobiol Aging. 2004;25:1263–72. [PubMed: 15465622]

[24]. Cataldo AM, Peterhoff CM, Troncoso JC, Gomez-Isla T, Hyman BT, Nixon RA. Endocytic pathway abnormalities precede amyloid beta deposition in sporadic Alzheimer's disease and Down syndrome: differential effects of APOE genotype and presenilin mutations. Am J Pathol. 2000;157:277–86. [PubMed: 10880397]

[25]. Martini AC, Helman AM, McCarty KL, Lott IT, Doran E, Schmitt FA, et al. Distribution of microglial phenotypes as a function of age and Alzheimer's disease neuropathology in the brains of people with Down syndrome. Alzheimers Dement (Amst). 2020;12:e12113. [PubMed: 33088896]

[26]. Sinai A, Mokrysz C, Bernal J, Bohnen I, Bonell S, Courtenay K, et al. Predictors of Age of Diagnosis and Survival of Alzheimer's Disease in Down Syndrome. J Alzheimers Dis. 2018;61:717–28. [PubMed: 29226868]

[27]. Prasher VP, Farrer MJ, Kessling AM, Fisher EM, West RJ, Barber PC, et al. Molecular mapping of Alzheimer-type dementia in Down's syndrome. Ann Neurol. 1998;43:380–3. [PubMed: 9506555]

[28]. Doran E, Keator D, Head E, Phelan MJ, Kim R, Totoiu M, et al. Down Syndrome, Partial Trisomy 21, and Absence of Alzheimer's Disease: The Role of APP. J Alzheimers Dis. 2017;56:459–70. [PubMed: 27983553]

[29]. Cacace R, Sleegers K, Van Broeckhoven C. Molecular genetics of early-onset Alzheimer's disease revisited. Alzheimers Dement. 2016;12:733–48. [PubMed: 27016693]

[30]. Cabrejo L, Guyant-Marechal L, Laquerriere A, Vercelletto M, De la Fourniere F, Thomas-Anterion C, et al. Phenotype associated with APP duplication in five families. Brain. 2006;129:2966–76. [PubMed: 16959815]

[31]. Sleegers K, Brouwers N, Gijselinck I, Theuns J, Goossens D, Wauters J, et al. APP duplication is sufficient to cause early onset Alzheimer's dementia with cerebral amyloid angiopathy. Brain. 2006;129:2977–83. [PubMed: 16921174]

[32]. Rumble B, Retallack R, Hilbich C, Simms G, Multhaup G, Martins R, et al. Amyloid A4 protein and its precursor in Down's syndrome and Alzheimer's disease. N Engl J Med. 1989;320:1446–52. [PubMed: 2566117]

[33]. Oyama F, Cairns NJ, Shimada H, Oyama R, Titani K, Ihara Y. Down's syndrome: up-regulation of beta-amyloid protein precursor and tau mRNAs and their defective coordination. J Neurochem. 1994;62:1062–6. [PubMed: 8113792]

[34]. Holler CJ, Webb RL, Laux AL, Beckett TL, Niedowicz DM, Ahmed RR, et al. BACE2 expression increases in human neurodegenerative disease. Am J Pathol. 2012;180:337–50. [PubMed: 22074738]

[35]. Griffin WST, Sheng JG, McKenzie JE, Royston MC, Gentleman SM, Brumback RA, et al. Life-long overexpression of S100β in Down's syndrome: implications for Alzheimer pathogenesis. Neurobiol Aging. 1998;19:401–5. [PubMed: 9880042]

[36]. Hirayama A, Horikoshi Y, Maeda M, Ito M, Takashima S. Characteristic developmental expression of amyloid β40, 42 and 43 in patients with Down syndrome. Brain and Development. 2003;25:180–5. [PubMed: 12689696]

[37]. Nistor M, Don M, Parekh M, Sarsoza F, Goodus M, Lopez GE, et al. Alpha- and beta-secretase activity as a function of age and beta-amyloid in Down syndrome and normal brain. Neurobiol Aging. 2007;28:1493–506. [PubMed: 16904243]

[38]. Cheon MS, Dierssen M, Kim SH, Lubec G. Protein expression of BACE1, BACE2 and APP in Down syndrome brains. Amino Acids. 2008;35:339–43. [PubMed: 18163181]

[39]. Rafii MS, Kleschevnikov AM, Sawa M, Mobley WC. Down syndrome. Handb Clin Neurol. 2019;167:321–36. [PubMed: 31753140]

[40]. Lemere CA, Blusztajn JK, Yamaguchi H, Wisniewski T, Saido TC, Selkoe DJ. Sequence of deposition of heterogeneous amyloid beta-peptides and APO E in Down syndrome: implications for initial events in amyloid plaque formation. Neurobiol Dis. 1996;3:16–32. [PubMed: 9173910]

[41]. Teller JK, Russo C, DeBusk LM, Angelini G, Zaccheo D, Dagna-Bricarelli F, et al. Presence of soluble amyloid beta-peptide precedes amyloid plaque formation in Down's syndrome. Nat Med. 1996;2:93–5. [PubMed: 8564851]

[42]. Glenner G, Wong C. Alzheimer's disease: initial report of the purification and characterization of a novel cerebrovascular amyloid protein. BiochemBiophysResCommun. 1984;12:885–90.

[43]. Schupf N, Patel B, Silverman W, Zigman WB, Zhong N, Tycko B, et al. Elevated plasma amyloid beta-peptide 1–42 and onset of dementia in adults with Down syndrome. Neurosci Lett. 2001;301:199–203. [PubMed: 11257432]

[44]. Mori C, Spooner ET, Wisniewsk KE, Wisniewski TM, Yamaguch H, Saido TC, et al. Intraneuronal Abeta42 accumulation in Down syndrome brain. Amyloid. 2002;9:88–102. [PubMed: 12440481]

[45]. Head E, Doran E, Nistor M, Hill M, Schmitt FA, Haier RJ, et al. Plasma amyloid-beta as a function of age, level of intellectual disability, and presence of dementia in Down syndrome. J Alzheimers Dis. 2011;23:399–409. [PubMed: 21116050]

[46]. Rafii MS, Wishnek H, Brewer JB, Donohue MC, Ness S, Mobley WC, et al. The down syndrome biomarker initiative (DSBI) pilot: proof of concept for deep phenotyping of Alzheimer's disease biomarkers in down syndrome. Frontiers in behavioral neuroscience. 2015;9:239. [PubMed: 26441570]

[47]. Fortea J, Carmona-Iragui M, Benejam B, Fernandez S, Videla L, Barroeta I, et al. Plasma and CSF biomarkers for the diagnosis of Alzheimer's disease in adults with Down syndrome: a cross-sectional study. Lancet Neurol. 2018;17:860–9. [PubMed: 30172624]

[48]. Startin CM, Ashton NJ, Hamburg S, Hithersay R, Wiseman FK, Mok KY, et al. Plasma biomarkers for amyloid, tau, and cytokines in Down syndrome and sporadic Alzheimer's disease. Alzheimers Res Ther. 2019;11:26. [PubMed: 30902060]

[49]. Davidson YS, Robinson A, Prasher VP, Mann DMA. The age of onset and evolution of Braak tangle stage and Thal amyloid pathology of Alzheimer's disease in individuals with Down syndrome. Acta Neuropathol Commun. 2018;6:56. [PubMed: 29973279]

[50]. Fortea J, Vilaplana E, Carmona-Iragui M, Benejam B, Videla L, Barroeta I, et al. Clinical and biomarker changes of Alzheimer's disease in adults with Down syndrome: a cross-sectional study. Lancet. 2020;395:1988–97. [PubMed: 32593336]

[51]. National Down Syndrome Society. Alzheimer's disease and Down syndrome. https://www.ndss.org/resources/alzheimers/ Last accessed: 2/15/2021

[52]. Hebert LE, Weuve J, Scherr PA, Evans DA. Alzheimer disease in the United States (2010–2050) estimated using the 2010 census. Neurology. 2013;80:1778–83. [PubMed: 23390181]

[53]. The National Institute on Aging aRIW, Neuropathological GoDCft, Disease AoAs. Consensus recommendations for the postmortem diagnosis of Alzheimer's disease. The National Institute on Aging, and Reagan Institute Working Group on Diagnostic Criteria for the Neuropathological Assessment of Alzheimer's Disease. Neurobiol Aging. 1997;18:S1–2. [PubMed: 9330978]

[54]. Mirra SS, Heyman A, McKeel D, Sumi SM, Crain BJ, Brownlee LM, et al. The Consortium to Establish a Registry for Alzheimer's Disease (CERAD). Part II. Standardization of the neuropathologic assessment of Alzheimer's disease. Neurology. 1991;41:479–86. [PubMed: 2011243]

[55]. Thal DR, Rub U, Orantes M, Braak H. Phases of A beta-deposition in the human brain and its relevance for the development of AD. Neurology. 2002;58:1791–800. [PubMed: 12084879]

[56]. Braak H, Braak E. Neuropathological stageing of Alzheimer-related changes. Acta Neuropathol. 1991;82:239–59. [PubMed: 1759558]

[57]. Yu T, Li Z, Jia Z, Clapcote SJ, Liu C, Li S, et al. A mouse model of Down syndrome trisomic for all human chromosome 21 syntenic regions. Hum Mol Genet. 2010;19:2780–91. [PubMed: 20442137]

[58]. Yu T, Liu C, Belichenko P, Clapcote SJ, Li S, Pao A, et al. Effects of individual segmental trisomies of human chromosome 21 syntenic regions on hippocampal long-term potentiation and cognitive behaviors in mice. Brain Res. 2010;1366:162–71. [PubMed: 20932954]

[59]. Goodliffe JW, Olmos-Serrano JL, Aziz NM, Pennings JL, Guedj F, Bianchi DW, et al. Absence of Prenatal Forebrain Defects in the Dp(16)1Yey/+ Mouse Model of Down Syndrome. J Neurosci. 2016;36:2926–44. [PubMed: 26961948]

[60]. Zheng H, Jiang M, Trumbauer ME, Hopkins R, Sirinathsinghji DJ, Stevens KA, et al. Mice deficient for the amyloid precursor protein gene. Ann N Y Acad Sci. 1996;777:421–6. [PubMed: 8624124]

[61]. Logsdon BA, Perumal TM, Swarup V, Wang M, Funk C, Gaiteri C, et al. Meta-analysis of the human brain transcriptome identifies heterogeneity across human AD coexpression modules robust to sample collection and methodological approach bioRxiv doi: 10.1101/510420 2019.

[62]. Overk CR, Kelley CM, Mufson EJ. Brainstem Alzheimer's-like pathology in the triple transgenic mouse model of Alzheimer's disease. Neurobiology of disease. 2009;35:415–25. [PubMed: 19524671]

[63]. Spencer B, Desplats PA, Overk CR, Valera-Martin E, Rissman RA, Wu C, et al. Reducing Endogenous alpha-Synuclein Mitigates the Degeneration of Selective Neuronal Populations in an Alzheimer's Disease Transgenic Mouse Model. J Neurosci. 2016;36:7971–84. [PubMed: 27466341]

[64]. Zoltowska KM, Berezovska O. Dynamic Nature of presenilin1/gamma-Secretase: Implication for Alzheimer's Disease Pathogenesis. Mol Neurobiol. 2018;55:2275–84. [PubMed: 28332150]

[65]. Tarasoff-Conway JM, Carare RO, Osorio RS, Glodzik L, Butler T, Fieremans E, et al. Clearance systems in the brain--implications for Alzheimer diseaser. Nat Rev Neurol. 2016;12:248. [PubMed: 27020556]

[66]. Paterson RW, Gabelle A, Lucey BP, Barthelemy NR, Leckey CA, Hirtz C, et al. SILK studies - capturing the turnover of proteins linked to neurodegenerative diseases. Nat Rev Neurol. 2019;15:419–27. [PubMed: 31222062]

[67]. Wildsmith KR, Basak JM, Patterson BW, Pyatkivskyy Y, Kim J, Yarasheski KE, et al. In vivo human apolipoprotein E isoform fractional turnover rates in the CNS. PLoS One. 2012;7:e38013. [PubMed: 22675504]

[68]. Bateman RJ, Siemers ER, Mawuenyega KG, Wen G, Browning KR, Sigurdson WC, et al. A gamma-secretase inhibitor decreases amyloid-beta production in the central nervous system. Ann Neurol. 2009;66:48–54. [PubMed: 19360898]

[69]. Janelidze S, Zetterberg H, Mattsson N, Palmqvist S, Vanderstichele H, Lindberg O, et al. CSF Abeta42/Abeta40 and Abeta42/Abeta38 ratios: better diagnostic markers of Alzheimer disease. Ann Clin Transl Neurol. 2016;3:154–65. [PubMed: 27042676]

[70]. Ferguson SA, Panos JJ, Sloper D, Varma V. Neurodegenerative Markers are Increased in Postmortem BA21 Tissue from African Americans with Alzheimer's Disease. J Alzheimers Dis. 2017;59:57–66. [PubMed: 28582866]

[71]. Funato H, Yoshimura M, Kusui K, Tamaoka A, Ishikawa K, Ohkoshi N, et al. Quantitation of amyloid beta-protein (A beta) in the cortex during aging and in Alzheimer's disease. Am J Pathol. 1998;152:1633–40. [PubMed: 9626067]

[72]. Pelleri MC, Cicchini E, Locatelli C, Vitale L, Caracausi M, Piovesan A, et al. Systematic reanalysis of partial trisomy 21 cases with or without Down syndrome suggests a small region on 21q22.13 as critical to the phenotype. Hum Mol Genet. 2016;25:2525–38. [PubMed: 27106104]

[73]. Pelleri MC, Cicchini E, Petersen MB, Tranebjaerg L, Mattina T, Magini P, et al. Partial trisomy 21 map: Ten cases further supporting the highly restricted Down syndrome critical region (HR-DSCR) on human chromosome 21. Molecular genetics & genomic medicine. 2019;7:e797. [PubMed: 31237416]

[74]. Lyle R, Bena F, Gagos S, Gehrig C, Lopez G, Schinzel A, et al. Genotype-phenotype correlations in Down syndrome identified by array CGH in 30 cases of partial trisomy and partial monosomy chromosome 21. Eur J Hum Genet. 2009;17:454–66. [PubMed: 19002211]

[75]. Korbel JO, Tirosh-Wagner T, Urban AE, Chen XN, Kasowski M, Dai L, et al. The genetic architecture of Down syndrome phenotypes revealed by high-resolution analysis of human segmental trisomies. Proc Natl Acad Sci U S A. 2009;106:12031–6. [PubMed: 19597142]

[76]. Nhan HS, Chiang K, Koo EH. The multifaceted nature of amyloid precursor protein and its proteolytic fragments: friends and foes. Acta Neuropathol. 2015;129:1–19. [PubMed: 25287911]

[77]. Arriagada P, Growdon J, Hedley-Whyte E, Hyman B. Neurofibrillary tangles but not senile plaques parallel duration and severity of Alzheimer's disease. Neurology. 1992;42:631–9. [PubMed: 1549228]

[78]. Chen XQ, Mobley WC. Alzheimer Disease Pathogenesis: Insights From Molecular and Cellular Biology Studies of Oligomeric Abeta and Tau Species. Front Neurosci. 2019;13:659. [PubMed: 31293377]

[79]. Zhou Y, Shi J, Chu D, Hu W, Guan Z, Gong CX, et al. Relevance of Phosphorylation and Truncation of Tau to the Etiopathogenesis of Alzheimer's Disease. Front Aging Neurosci. 2018;10:27. [PubMed: 29472853]

[80]. Ryoo SR, Jeong HK, Radnaabazar C, Yoo JJ, Cho HJ, Lee HW, et al. DYRK1A-mediated hyperphosphorylation of Tau. A functional link between Down syndrome and Alzheimer disease. J Biol Chem. 2007;282:34850–7. [PubMed: 17906291]

[81]. Gupta M, Dhanasekaran AR, Gardiner KJ. Mouse models of Down syndrome: gene content and consequences. Mamm Genome. 2016;27:538–55. [PubMed: 27538963]

[82]. Bennett DA, Schneider JA, Arvanitakis Z, Wilson RS. Overview and findings from the religious orders study. Curr Alzheimer Res. 2012;9:628–45. [PubMed: 22471860]

[83]. Allen M, Carrasquillo MM, Funk C, Heavner BD, Zou F, Younkin CS, et al. Human whole genome genotype and transcriptome data for Alzheimer's and other neurodegenerative diseases. Scientific data. 2016;3:160089. [PubMed: 27727239]

[84]. Wang M, Beckmann ND, Roussos P, Wang E, Zhou X, Wang Q, et al. The Mount Sinai cohort of large-scale genomic, transcriptomic and proteomic data in Alzheimer's disease. Scientific data. 2018;5:180185. [PubMed: 30204156]

[85]. Gomez M, Germain D. Cross talk between SOD1 and the mitochondrial UPR in cancer and neurodegeneration. Mol Cell Neurosci. 2019;98:12–8. [PubMed: 31028834]

[86]. Herrero-Garcia E, O'Bryan JP. Intersectin scaffold proteins and their role in cell signaling and endocytosis. Biochimica et biophysica acta Molecular cell research. 2017;1864:23–30. [PubMed: 27746143]

[87]. Lott IT. Neurological phenotypes for Down syndrome across the life span. Prog Brain Res. 2012;197:101–21. [PubMed: 22541290]

[88]. von Gunten A, Kovari E, Bussiere T, Rivara CB, Gold G, Bouras C, et al. Cognitive impact of neuronal pathology in the entorhinal cortex and CA1 field in Alzheimer's disease. Neurobiol Aging. 2006;27:270–7. [PubMed: 16399212]

[89]. Sadowski M, Wisniewski HM, Tarnawski M, Kozlowski PB, Lach B, Wegiel J. Entorhinal cortex of aged subjects with Down's syndrome shows severe neuronal loss caused by neurofibrillary pathology. Acta Neuropathol. 1999;97:156–64. [PubMed: 9928826]

[90]. Weinshenker D. Functional consequences of locus coeruleus degeneration in Alzheimer's disease. Curr Alzheimer Res. 2008;5:342–5. [PubMed: 18537547]

[91]. German DC, Manaye KF, White CL 3rd, Woodward DJ, McIntire DD, Smith WK, et al. Disease-specific patterns of locus coeruleus cell loss. Ann Neurol. 1992;32:667–76. [PubMed: 1449247]

[92]. Schliebs R, Arendt T. The cholinergic system in aging and neuronal degeneration. Behav Brain Res. 2011;221:555–63. [PubMed: 21145918]

[93]. Casanova MF, Walker LC, Whitehouse PJ, Price DL. Abnormalities of the nucleus basalis in Down's syndrome. Ann Neurol. 1985;18:310–3. [PubMed: 2932050]

[94]. Uchihara T, Nakamura A, Yamazaki M, Mori O. Evolution from pretangle neurons to neurofibrillary tangles monitored by thiazin red combined with Gallyas method and double immunofluorescence. Acta Neuropathol. 2001;101:535–9. [PubMed: 11515780]

[95]. Sendera TJ, Ma SY, Jaffar S, Kozlowski PB, Kordower JH, Mawal Y, et al. Reduction in TrkA-immunoreactive neurons is not associated with an overexpression of galaninergic fibers within the nucleus basalis in Down's syndrome. J Neurochem. 2000;74:1185–96. [PubMed: 10693951]

[96]. Mandrekar-Colucci S, Landreth GE. Microglia and inflammation in Alzheimer's disease. CNS Neurol Disord Drug Targets. 2010;9:156–67. [PubMed: 20205644]

[97]. De Strooper B, Karran E. The Cellular Phase of Alzheimer's Disease. Cell. 2016;164:603–15. [PubMed: 26871627]

[98]. Pinto B, Morelli G, Rastogi M, Savardi A, Fumagalli A, Petretto A, et al. Rescuing Over-activated Microglia Restores Cognitive Performance in Juvenile Animals of the Dp(16) Mouse Model of Down Syndrome. Neuron. 2020;108:887–904 e12. [PubMed: 33027640]

[99]. Liu CY, Yang Y, Ju WN, Wang X, Zhang HL. Emerging Roles of Astrocytes in Neuro-Vascular Unit and the Tripartite Synapse With Emphasis on Reactive Gliosis in the Context of Alzheimer's Disease. Front Cell Neurosci. 2018;12:193. [PubMed: 30042661]

[100]. Arnold SE, Franz BR, Trojanowski JQ, Moberg PJ, Gur RE. Glial fibrillary acidic protein-immunoreactive astrocytosis in elderly patients with schizophrenia and dementia. Acta Neuropathol. 1996;91:269–77. [PubMed: 8834539]

[101]. Hof PR, Bouras C, Perl DP, Sparks DL, Mehta N, Morrison JH. Age-related distribution of neuropathologic changes in the cerebral cortex of patients with Down's syndrome. Quantitative regional analysis and comparison with Alzheimer's disease. Arch Neurol. 1995;52:379–91. [PubMed: 7710374]

[102]. Hyman BT, Marzloff K, Arriagada PV. The lack of accumulation of senile plaques or amyloid burden in Alzheimer's disease suggests a dynamic balance between amyloid deposition and resolution. J Neuropathol Exp Neurol. 1993;52:594–600. [PubMed: 8229078]

[103]. Riedel BC, Thompson PM, Brinton RD. Age, APOE and sex: Triad of risk of Alzheimer's disease. J Steroid Biochem Mol Biol. 2016;160:134–47. [PubMed: 26969397]

[104]. Bayen E, Possin KL, Chen Y, Cleret de Langavant L, Yaffe K. Prevalence of Aging, Dementia, and Multimorbidity in Older Adults With Down Syndrome. JAMA Neurol. 2018;75:1399–406. [PubMed: 30032260]

[105]. Coppus A, Evenhuis H, Verberne GJ, Visser F, van Gool P, Eikelenboom P, et al. Dementia and mortality in persons with Down's syndrome. J Intellect Disabil Res. 2006;50:768–77. [PubMed: 16961706]

[106]. Lai F, Kammann E, Rebeck GW, Anderson A, Chen Y, Nixon RA. APOE genotype and gender effects on Alzheimer disease in 100 adults with Down syndrome. Neurology. 1999;53:331–6. [PubMed: 10430422]

[107]. Schupf N, Pang D, Patel BN, Silverman W, Schubert R, Lai F, et al. Onset of dementia is associated with age at menopause in women with Down's syndrome. Ann Neurol. 2003;54:433–8. [PubMed: 14520653]

[108]. Schupf N, Zigman W, Kapell D, Lee JH, Kline J, Levin B. Early menopause in women with Down's syndrome. J Intellect Disabil Res. 1997;41 (Pt 3):264–7. [PubMed: 9219076]

[109]. Lai F, Mhatre PG, Yang Y, Wang MC, Schupf N, Rosas HD. Sex differences in risk of Alzheimer's disease in adults with Down syndrome. Alzheimers Dement (Amst). 2020;12:e12084. [PubMed: 32995462]

[110]. Pike CJ. Sex and the development of Alzheimer's disease. J Neurosci Res. 2017;95:671–80. [PubMed: 27870425]

[111]. Rettberg JR, Yao J, Brinton RD. Estrogen: a master regulator of bioenergetic systems in the brain and body. Front Neuroendocrinol. 2014;35:8–30. [PubMed: 23994581]

[112]. Sambamurti K, Kinsey R, Maloney B, Ge YW, Lahiri DK. Gene structure and organization of the human beta-secretase (BACE) promoter. FASEB J. 2004;18:1034–6. [PubMed: 15059975]

[113]. Barron AM, Pike CJ. Sex hormones, aging, and Alzheimer's disease. Front Biosci (Elite Ed). 2012;4:976–97. [PubMed: 22201929]

[114]. Liang K, Yang L, Yin C, Xiao Z, Zhang J, Liu Y, et al. Estrogen stimulates degradation of beta-amyloid peptide by up-regulating neprilysin. J Biol Chem. 2010;285:935–42. [PubMed: 19897485]

[115]. Salehi A, Delcroix JD, Belichenko PV, Zhan K, Wu C, Valletta JS, et al. Increased App expression in a mouse model of Down's syndrome disrupts NGF transport and causes cholinergic neuron degeneration. Neuron. 2006;51:29–42. [PubMed: 16815330]

[116]. Salehi A, Faizi M, Colas D, Valletta J, Laguna J, Takimoto-Kimura R, et al. Restoration of norepinephrine-modulated contextual memory in a mouse model of Down syndrome. Sci Transl Med. 2009;1:7ra17.

[117]. Brendza RP, Bacskai BJ, Cirrito JR, Simmons KA, Skoch JM, Klunk WE, et al. Anti-Abeta antibody treatment promotes the rapid recovery of amyloid-associated neuritic dystrophy in PDAPP transgenic mice. The Journal of clinical investigation. 2005;115:428–33. [PubMed: 15668737]

[118]. Selkoe DJ, Hardy J. The amyloid hypothesis of Alzheimer's disease at 25 years. EMBO Mol Med. 2016;8:595–608. [PubMed: 27025652]

[119]. Wegiel J, Gong CX, Hwang YW. The role of DYRK1A in neurodegenerative diseases. FEBS J. 2011;278:236–45. [PubMed: 21156028]

[120]. Kay LJ, Smulders-Srinivasan TK, Soundararajan M. Understanding the Multifaceted Role of Human Down Syndrome Kinase DYRK1A. Advances in protein chemistry and structural biology. 2016;105:127–71. [PubMed: 27567487]

[121]. De Strooper B, Simons M, Multhaup G, Van Leuven F, Beyreuther K, Dotti CG. Production of intracellular amyloid-containing fragments in hippocampal neurons expressing human amyloid precursor protein and protection against amyloidogenesis by subtle amino acid substitutions in the rodent sequence. EMBO J. 1995;14:4932–8. [PubMed: 7588622]

[122]. Mucke L, Masliah E, Yu GQ, Mallory M, Rockenstein EM, Tatsuno G, et al. High-level neuronal expression of abeta 1–42 in wild-type human amyloid protein precursor transgenic mice: synaptotoxicity without plaque formation. J Neurosci. 2000;20:4050–8. [PubMed: 10818140]

[123]. Kazuki Y, Gao FJ, Li Y, Moyer AJ, Devenney B, Hiramatsu K, et al. A non-mosaic transchromosomic mouse model of down syndrome carrying the long arm of human chromosome 21. Elife. 2020;9.

[124]. Mathys H, Davila-Velderrain J, Peng Z, Gao F, Mohammadi S, Young JZ, et al. Single-cell transcriptomic analysis of Alzheimer's disease. Nature. 2019;570:332–7. [PubMed: 31042697]

[125]. Colman RJ. Non-human primates as a model for aging. Biochimica et biophysica acta Molecular basis of disease. 2018;1864:2733–41. [PubMed: 28729086]

[126]. Miller CT, Freiwald WA, Leopold DA, Mitchell JF, Silva AC, Wang X. Marmosets: A Neuroscientific Model of Human Social Behavior. Neuron. 2016;90:219–33. [PubMed: 27100195]

[127]. Park J, Wetzel I, Marriott I, Dreau D, D'Avanzo C, Kim DY, et al. A 3D human triculture system modeling neurodegeneration and neuroinflammation in Alzheimer's disease. Nature neuroscience. 2018;21:941–51. [PubMed: 29950669]

[128]. Papaspyropoulos A, Tsolaki M, Foroglou N, Pantazaki AA. Modeling and Targeting Alzheimer's Disease With Organoids. Frontiers in pharmacology. 2020;11:396. [PubMed: 32300301]

[129]. Gough G, O'Brien NL, Alic I, Goh PA, Yeap YJ, Groet J, et al. Modeling Down syndrome in cells: From stem cells to organoids. Prog Brain Res. 2020;251:55–90. [PubMed: 32057312]

[130]. Alic I, Goh PA, Murray A, Portelius E, Gkanatsiou E, Gough G, et al. Patient-specific Alzheimer-like pathology in trisomy 21 cerebral organoids reveals BACE2 as a gene dose-sensitive AD suppressor in human brain. Mol Psychiatry. 2020.

[131]. Head E, Phelan MJ, Doran E, Kim RC, Poon WW, Schmitt FA, et al. Cerebrovascular pathology in Down syndrome and Alzheimer disease. Acta neuropathologica communications. 2017;5:93. [PubMed: 29195510]

[132]. Pham MT, Pollock KM, Rose MD, Cary WA, Stewart HR, Zhou P, et al. Generation of human vascularized brain organoids. Neuroreport. 2018;29:588–93. [PubMed: 29570159]

[133]. Nixon RA. Amyloid precursor protein and endosomal-lysosomal dysfunction in Alzheimer's disease: inseparable partners in a multifactorial disease. FASEB J. 2017;31:2729–43. [PubMed: 28663518]

[134]. Chen XQ, Sawa M, Mobley WC. Dysregulation of neurotrophin signaling in the pathogenesis of Alzheimer disease and of Alzheimer disease in Down syndrome. Free radical biology & medicine. 2018;114:52–61. [PubMed: 29031834]

[135]. Pensalfini A, Kim S, Subbanna S, Bleiwas C, Goulbourne CN, Stavrides PH, et al. Endosomal Dysfunction Induced by Directly Overactivating Rab5 Recapitulates Prodromal and Neurodegenerative Features of Alzheimer's Disease. Cell Rep. 2020;33:108420. [PubMed: 33238112]

[136]. Colacurcio DJ, Pensalfini A, Jiang Y, Nixon RA. Dysfunction of autophagy and endosomal-lysosomal pathways: Roles in pathogenesis of Down syndrome and Alzheimer's Disease. Free radical biology & medicine. 2018;114:40–51. [PubMed: 28988799]

[137]. Selkoe DJ, Yamazaki T, Citron M, Podlisny MB, Koo EH, Teplow DB, et al. The role of APP processing and trafficking pathways in the formation of amyloid beta-protein. Ann N Y Acad Sci. 1996;777:57–64. [PubMed: 8624127]

[138]. Xu W, Weissmiller AM, White JA 2nd, Fang, Wang, Wu Y, et al. Amyloid precursor protein-mediated endocytic pathway disruption induces axonal dysfunction and neurodegeneration. J Clin Invest. 2016;126:1815–33. [PubMed: 27064279]

[139]. Kim S, Sato Y, Mohan PS, Peterhoff C, Pensalfini A, Rigoglioso A, et al. Evidence that the rab5 effector APPL1 mediates APP-betaCTF-induced dysfunction of endosomes in Down syndrome and Alzheimer's disease. Mol Psychiatry. 2016;21:707–16. [PubMed: 26194181]

[140]. Jiang Y, Mullaney KA, Peterhoff CM, Che S, Schmidt SD, Boyer-Boiteau A, et al. Alzheimer's-related endosome dysfunction in Down syndrome is Abeta-independent but requires APP and is reversed by BACE-1 inhibition. Proc Natl Acad Sci U S A. 2010;107:1630–5. [PubMed: 20080541]

[141]. Hung COY, Livesey FJ. Altered gamma-Secretase Processing of APP Disrupts Lysosome and Autophagosome Function in Monogenic Alzheimer's Disease. Cell reports. 2018;25:3647–60 e2. [PubMed: 30590039]

[142]. Kwart D, Gregg A, Scheckel C, Murphy EA, Paquet D, Duffield M, et al. A Large Panel of Isogenic APP and PSEN1 Mutant Human iPSC Neurons Reveals Shared Endosomal

Abnormalities Mediated by APP beta-CTFs, Not Abeta. Neuron. 2019;104:1022. [PubMed: 31805257]

[143]. Israel MA, Yuan SH, Bardy C, Reyna SM, Mu Y, Herrera C, et al. Probing sporadic and familial Alzheimer's disease using induced pluripotent stem cells. Nature. 2012;482:216–20. [PubMed: 22278060]

[144]. Chen XQ, Salehi A, Pearn ML, Overk C, Nguyen PD, Kleschevnikov AM, et al. Targeting increased levels of APP in Down syndrome: Posiphen-mediated reductions in APP and its products reverse endosomal phenotypes in the Ts65Dn mouse model. Alzheimer's & dementia : the journal of the Alzheimer's Association. 2021;17:271–92.

[145]. Sofroniew MV, Howe CL, Mobley WC. Nerve growth factor signaling, neuroprotection, and neural repair. Annu Rev Neurosci. 2001;24:1217–81. [PubMed: 11520933]

[146]. Schoch KM, Miller TM. Antisense Oligonucleotides: Translation from Mouse Models to Human Neurodegenerative Diseases. Neuron. 2017;94:1056–70. [PubMed: 28641106]

[147]. Silva AC, Lobo DD, Martins IM, Lopes SM, Henriques C, Duarte SP, et al. Antisense oligonucleotide therapeutics in neurodegenerative diseases: the case of polyglutamine disorders. Brain. 2020;143:407–29. [PubMed: 31738395]

[148]. Sawa M, Zhao H, Kordasiewicz H, Fitzsimmons B, Derse D, Becker A. APP-directed antisense oligonucleotides reduced APP gene expression in mouse models of Down Syndrome. Proceedings of the 48th annual meeting of the Society for Neurosciences. San Diego, CA2018.

[149]. Kumar-Singh S, Dewachter I, Moechars D, Lubke U, De Jonghe C, Ceuterick C, et al. Behavioral disturbances without amyloid deposits in mice overexpressing human amyloid precursor protein with Flemish (A692G) or Dutch (E693Q) mutation. Neurobiol Dis. 2000;7:9–22. [PubMed: 10671319]

[150]. Erickson MA, Niehoff ML, Farr SA, Morley JE, Dillman LA, Lynch KM, et al. Peripheral administration of antisense oligonucleotides targeting the amyloid-beta protein precursor reverses AbetaPP and LRP-1 overexpression in the aged SAMP8 mouse brain. Journal of Alzheimer's disease : JAD. 2012;28:951–60. [PubMed: 22179572]

[151]. Farr SA, Erickson MA, Niehoff ML, Banks WA, Morley JE. Central and peripheral administration of antisense oligonucleotide targeting amyloid-beta protein precursor improves learning and memory and reduces neuroinflammatory cytokines in Tg2576 (AbetaPPswe) mice. Journal of Alzheimer's disease : JAD. 2014;40:1005–16. [PubMed: 24577464]

[152]. Shyam R, Ren Y, Lee J, Braunstein KE, Mao HQ, Wong PC. Intraventricular Delivery of siRNA Nanoparticles to the Central Nervous System. Molecular therapy Nucleic acids. 2015;4:e242. [PubMed: 25965552]

[153]. Zhou Y, Zhu F, Liu Y, Zheng M, Wang Y, Zhang D, et al. Blood-brain barrier-penetrating siRNA nanomedicine for Alzheimer's disease therapy. Science advances. 2020;6.

[154]. Cummings J, Lee G, Ritter A, Sabbagh M, Zhong K. Alzheimer's disease drug development pipeline: 2020. Alzheimers Dement (N Y). 2020;6:e12050. [PubMed: 32695874]

[155]. Coric V, Salloway S, van Dyck CH, Dubois B, Andreasen N, Brody M, et al. Targeting Prodromal Alzheimer Disease With Avagacestat: A Randomized Clinical Trial. JAMA neurology. 2015;72:1324–33. [PubMed: 26414022]

[156]. Coric V, van Dyck CH, Salloway S, Andreasen N, Brody M, Richter RW, et al. Safety and tolerability of the gamma-secretase inhibitor avagacestat in a phase 2 study of mild to moderate Alzheimer disease. Archives of neurology. 2012;69:1430–40. [PubMed: 22892585]

[157]. Doody RS, Raman R, Farlow M, Iwatsubo T, Vellas B, Joffe S, et al. A phase 3 trial of semagacestat for treatment of Alzheimer's disease. The New England journal of medicine. 2013;369:341–50. [PubMed: 23883379]

[158]. Fleisher AS, Raman R, Siemers ER, Becerra L, Clark CM, Dean RA, et al. Phase 2 safety trial targeting amyloid beta production with a gamma-secretase inhibitor in Alzheimer disease. Arch Neurol. 2008;65:1031–8. [PubMed: 18695053]

[159]. Wagner SL, Zhang C, Cheng S, Nguyen P, Zhang X, Rynearson KD, et al. Soluble gamma-secretase modulators selectively inhibit the production of the 42-amino acid amyloid beta peptide variant and augment the production of multiple carboxy-truncated amyloid beta species. Biochemistry. 2014;53:702–13. [PubMed: 24401146]

[160]. Rynearson KD, Ponnusamy M, Prikhodko O, Xie Y, Zhang C, Nguyen P, et al. Preclinical validation of a potent gamma-secretase modulator for Alzheimer's disease prevention. The Journal of experimental medicine. 2021;218.

[161]. Belichenko PV, Madani R, Rey-Bellet L, Pihlgren M, Becker A, Plassard A, et al. An Anti-beta-Amyloid Vaccine for Treating Cognitive Deficits in a Mouse Model of Down Syndrome. PLoS One. 2016;11:e0152471. [PubMed: 27023444]

[162]. Loureiro JC, Pais MV, Stella F, Radanovic M, Teixeira AL, Forlenza OV, et al. Passive antiamyloid immunotherapy for Alzheimer's disease. Current opinion in psychiatry. 2020;33:284–91. [PubMed: 32040044]

[163]. van Dyck CH. Anti-Amyloid-beta Monoclonal Antibodies for Alzheimer's Disease: Pitfalls and Promise. Biol Psychiatry. 2018;83:311–9. [PubMed: 28967385]

[164]. Russo C, Saido TC, DeBusk LM, Tabaton M, Gambetti P, Teller JK. Heterogeneity of water-soluble amyloid beta-peptide in Alzheimer's disease and Down's syndrome brains. FEBS Lett. 1997;409:411–6. [PubMed: 9224700]

[165]. Ji L, Chauhan V, Mehta P, Wegiel J, Mehta S, Chauhan A. Relationship between proteolytically cleaved gelsolin and levels of amyloid-beta protein in the brains of Down syndrome subjects. J Alzheimers Dis. 2010;22:609–17. [PubMed: 20847428]

[166]. Miners JS, Morris S, Love S, Kehoe PG. Accumulation of insoluble amyloid-beta in down's syndrome is associated with increased BACE-1 and neprilysin activities. J Alzheimers Dis. 2011;23:101–8. [PubMed: 20930275]

[167]. Cenini G, Dowling AL, Beckett TL, Barone E, Mancuso C, Murphy MP, et al. Association between frontal cortex oxidative damage and beta-amyloid as a function of age in Down syndrome. Biochim Biophys Acta. 2012;1822:130–8. [PubMed: 22009041]

[168]. Abrahamson EE, Head E, Lott IT, Handen BL, Mufson EJ, Christian BT, et al. Neuropathological correlates of amyloid PET imaging in Down syndrome. Developmental neurobiology. 2019;79:750–66. [PubMed: 31379087]

[169]. Liu F, Liang Z, Wegiel J, Hwang YW, Iqbal K, Grundke-Iqbal I, et al. Overexpression of Dyrk1A contributes to neurofibrillary degeneration in Down syndrome. FASEB J. 2008;22:3224–33. [PubMed: 18509201]

[170]. Hanger DP, Brion JP, Gallo JM, Cairns NJ, Luthert PJ, Anderton BH. Tau in Alzheimer's disease and Down's syndrome is insoluble and abnormally phosphorylated. Biochem J. 1991;275 (Pt 1):99–104. [PubMed: 1826835]

[171]. Shi J, Zhang T, Zhou C, Chohan MO, Gu X, Wegiel J, et al. Increased dosage of Dyrk1A alters alternative splicing factor (ASF)-regulated alternative splicing of tau in Down syndrome. J Biol Chem. 2008;283:28660–9. [PubMed: 18658135]

[172]. Hyman B, West H, Rebeck G, Lai F, Mann D. Neuropathological changes in Down's syndrome hippocampal formation. ArchNeurol. 1995;52:373–8.

[173]. Mann DM, Esiri MM. The pattern of acquisition of plaques and tangles in the brains of patients under 50 years of age with Down's syndrome. J Neurol Sci. 1989;89:169–79. [PubMed: 2522541]

[174]. Lemoine L, Ledreux A, Mufson EJ, Perez SE, Simic G, Doran E, et al. Regional binding of tau and amyloid PET tracers in Down syndrome autopsy brain tissue. Molecular neurodegeneration. 2020;15:68. [PubMed: 33222700]

[175]. Flores-Aguilar L, Iulita MF, Kovecses O, Torres MD, Levi SM, Zhang Y, et al. Evolution of neuroinflammation across the lifespan of individuals with Down syndrome. Brain. 2020.

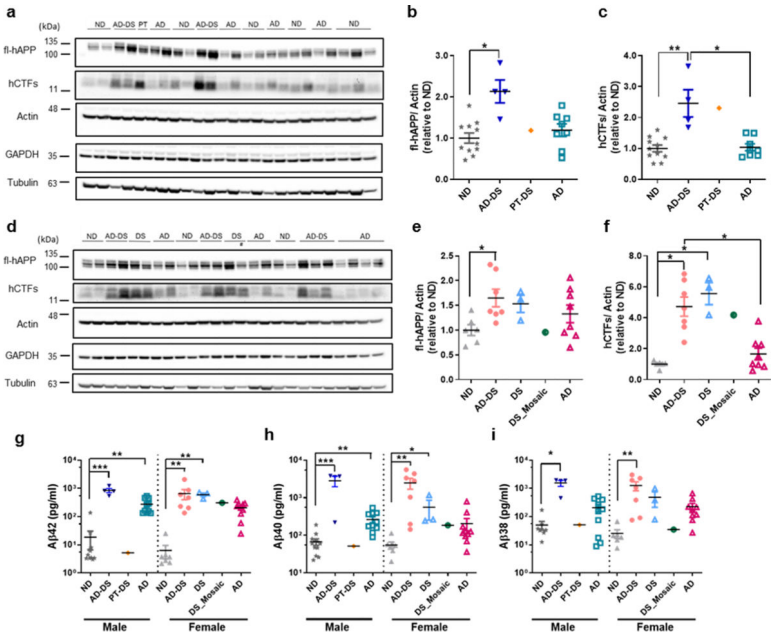

Figure 1. Analysis of human full-length (FL) APP (fl-hAPP) and its proteolytic products (hCTFs and Aβ42/40/38) in the postmortem brain tissues.

(a-f) Analysis of fl-hAPP and hCTFs in males and females; ND, AD-DS, PT-DS and DS cases were analyzed per sex; fl-hAPP and hCTFs were detected using anti-APP antibody (Y188, abcam); signal intensity of bands was quantified and normalized against β-Actin. (a-c) Analysis of male samples. (a) Representative images of western blots. (b) Quantification of fl-hAPP relative to Actin. Data are shown with respect to ND. (c) Quantification of hCTFs relative to Actin; data are shown with respect to ND. (d-f) Analysis of female samples. (d) Representative images of western blots. # Indicates the DS-Mosaic case. (e, f) Quantification of fl-hAPP, and hCTFs normalized with respect to Actin and expressed with respect to ND. (g-i) Measurement of concentrations of Aβ species (pg/ml): (g) Aβ42, (h) Aβ40 and (i) Aβ38. ND= non-demented; AD-DS = AD with DS, PT and PT-DS = DS with the partial trisomy; DS = DS without AD; AD = Alzheimer's disease. Statistical analyses were performed per sex. One way ANOVA (Kruskal-Wallis) test followed by Dunn's Multiple Comparison Test. * $p < 0.05$, ** $p < 0.01$, *** $p < 0.005$. For fl-hAPP/ hCTFs analysis: Male: ND, n = 11; AD-DS, n = 4; PT-DS, n = 1; AD, n = 8; Female: ND, n = 6; AD-DS, n = 7; DS, n = 4; AD, n = 8. For MSD analysis, Male: ND, n = 12; AD-DS, n = 4; PT-DS, n = 1; AD, n = 10. Female: ND, n = 8; AD-DS, n = 7; DS, n = 4; AD, n = 10.

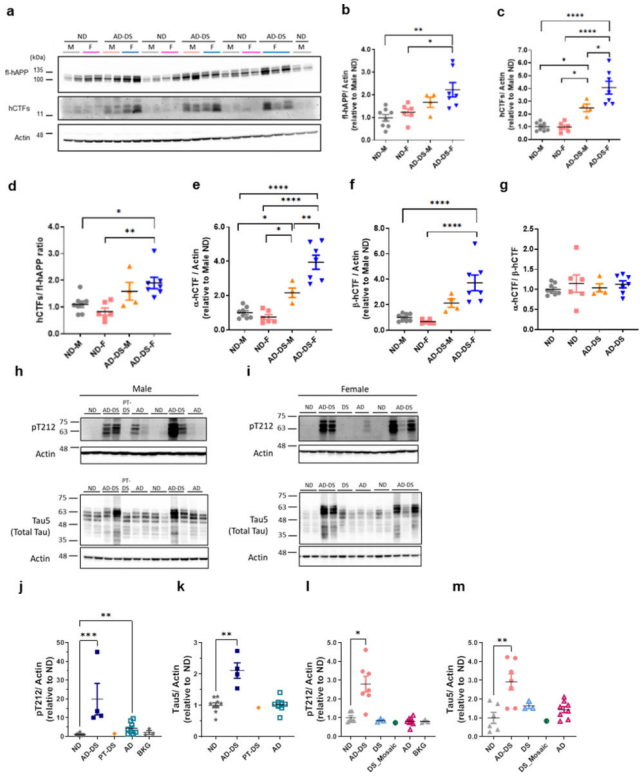

Figure 2. Differential processing of hAPP between males and females and gene-dose effects on pT212 in human postmortem brain tissues.

(a-f) Comparison of fl-hAPP and hCTFs levels in males and females. (a) Representative images of western blots. (b) Quantification of fl-hAPP relative to Actin normalized to ND males. (c) Quantification of hCTFs relative to actin, normalized to ND males. (d) h-CTFs relative to fl-hAPP. (e) Quantification of shorter hCTFs (α-hCTFs) relative to Actin, normalized to ND males. (f) Quantification of longer hCTFs (β-hCTFs) relative to Actin, normalized to ND males. (g) The ratio between shorter and longer hCTFs (α-/β-hCTFs). Two-way ANOVA followed by post-hoc Tukey's multiple comparisons test, * $p < 0.05$, **$p < 0.01$., ****$p < 0.001$. (h-l) Analysis of pT212 and total Tau levels. (h, i) Representative images of pT212 and Tau levels in males (left) and females (right). Actin serves as a loading control. (j-m) Quantification of pT212 and total Tau levels. Levels of pT212 in (j) males and (l) females. Data were normalized to Actin and shown with respect to ND. BKG: Randomly selected three ROIs with no signal are shown to indicate background signal levels. (k) Levels of total Tau in males. (m) Total tau in females. Kruskal-Wallis test followed by Dunn's Multiple Comparison Test, * $p < 0.05$, **$p < 0.01$, ***$p < 0.005$.

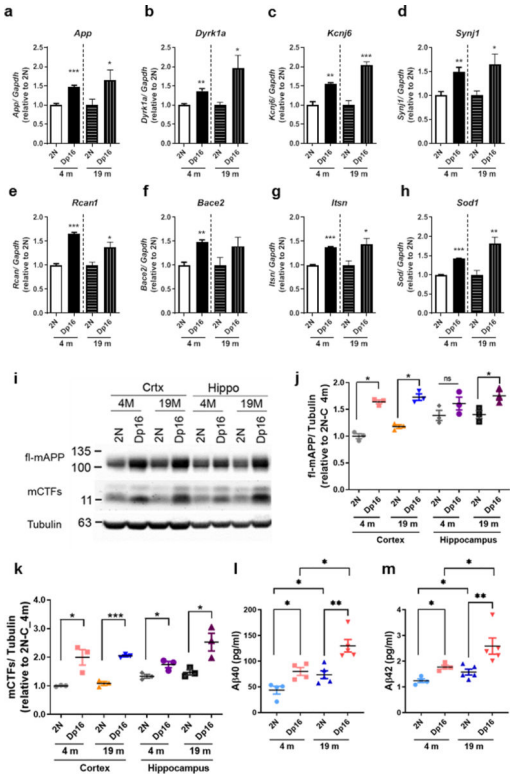

Figure 3. mRNA and Protein levels in Dp16 and 2N mice at 4 and 19 months.

(a-h) Transcriptional analyses of the genes on mouse Chromosome 16 at 4 and 19 months. mRNA levels of (a) *App*, (b) *Dyrk1a*, (c) *Kcnj6*, (d) *Synj1*, (e) *Rcan1*, (f) *Bace2*, (g) *Itsn1* and (h) *Sod1* were analyzed by qPCR. Expression levels were normalized to *Gapdh*. Relative values to 2N at each age are shown ± S.E.M. Two-tailed unpaired t-test: * $p < 0.05$, ** $p < 0.01$ and *** $p < 0.005$. n = 4 at 4 months for each genotype. n = 5 at 19 months for each genotype. (i-m) Quantification of protein levels of mouse full-length (fl) APP (fl-mAPP) and its proteolytic products (mCTFs and Aβ42/Aβ40) at 4 and 19 months in 2N and Dp16 mice. (i) Representative images of western blots. (j) Quantification of fl-mAPP normalized to Tubulin. (k) Quantification of mCTFs normalized to Tubulin and expressed relative to the 2N control. Data in i and k are shown as relative to the 2N cortex at 4 months. Mean ± S.E.M., two-tailed unpaired t-test performed between indicated groups, * $p < 0.05$, ** $p < 0.01$ and *** $p < 0.005$, n = 3 all samples. (l, m) Measurement of (l) Aβ40 and (m) Aβ42 in the cortex of 2N and Dp16 mice at 4 and 19 months. Mean (pg/ml) ± S.E.M., Two-tailed unpaired t-tests were conducted between the indicated groups: * $p < 0.05$, ** $p < 0.01$ and *** $p < 0.005$. Aβ40: n for 2N at 4 months = 4 and at 19 months = 5; n for Dp16 at 4 months = 4 and at 19 months = 5. Aβ42: n for 2N at 4 months = 4 and at 19 months = 5; n for Dp16 at 4 months = 4 and at 19 months = 5. As for Supplementary Table 2, the ratios between the amount of Aβ and the total protein lysate were calculated (i.e., mean average concentration of Aβ peptides in pg per mg total protein in the sample). The values are as follows: Aβ40: 2N at 4 months = 4.37, Dp16 at 4 months = 8.00, 2N at 19 months = 7.36, Dp16 at 19 months = 13.00; Aβ42: 2N at 4 months = 0.12, Dp16 at 4 months = 0.17, 2N at 19 months = 0.16, Dp16 at 19 months = 0.26.

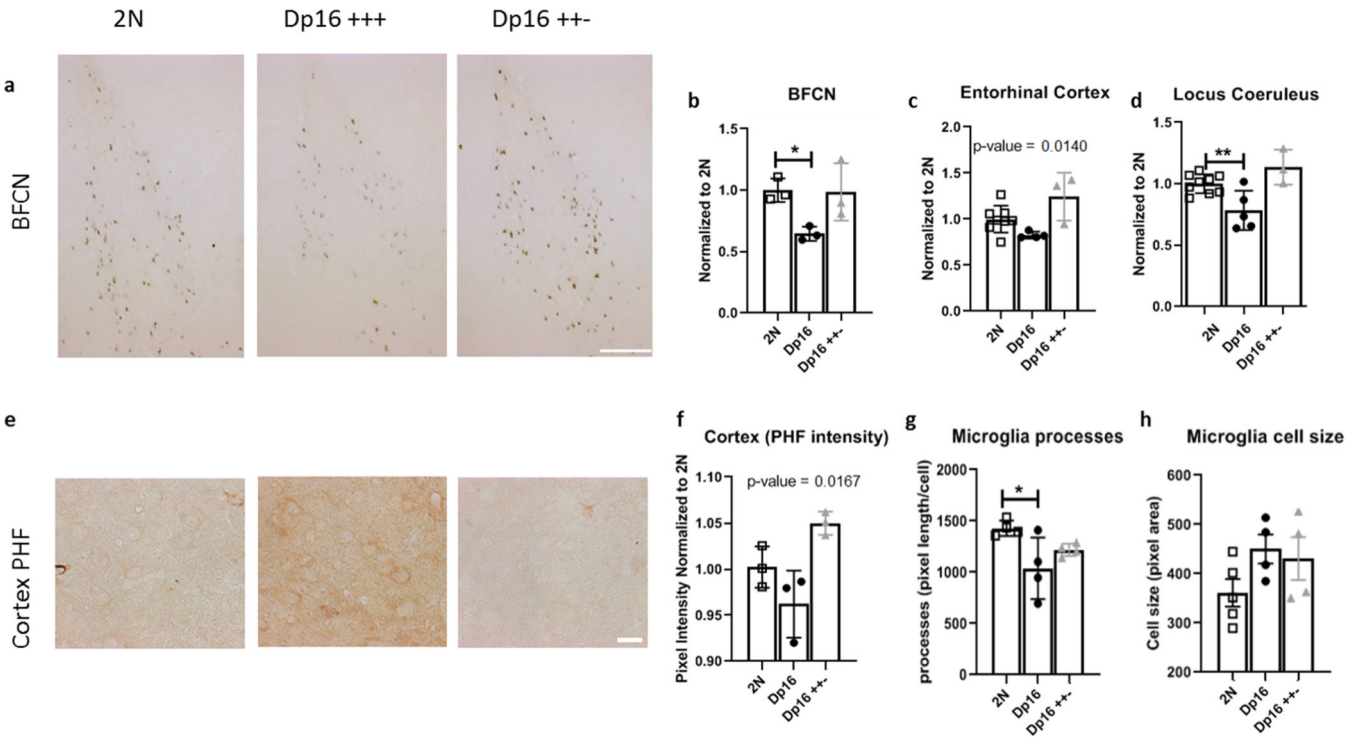

Figure 4. Histological studies of AD-relevant phenotypes in Dp16, Dp16(m*App* ++-), and 2N mice.

Dp16, Dp16 (m*App* ++-), and 2N mice were evaluated between 13 and 19 months of age. (a) Photomicrographs of medial septum BFCNs. Quantitation of the relative number of neurons normalized to 2N mice in the (b) medial septum, (c) entorhinal cortex layer 2/3, and (d) locus coeruleus. (e) Photomicrographs of PHF-immunoreactivity in the cortex. (f) Quantitation of the PHF-ir pixel intensity. Quantification of (g) IBA-1-positive microglial process length, and (h) IBA-1-positive microglial cell size in the cortex. Scale bars in a = 250 μm, e = 25 μm, Statistical analysis was performed using one-way ANOVA followed by Dunnett's post hoc analysis comparing all columns to 2N. * = p-value < 0.05; ** = p-value < 0.01. In panels (c) and (f) there was a statistically significant difference between groups; however, the post hoc analysis was unable to identify which comparison was significant. The p-value from the one-way ANOVA analysis is listed on the graph.

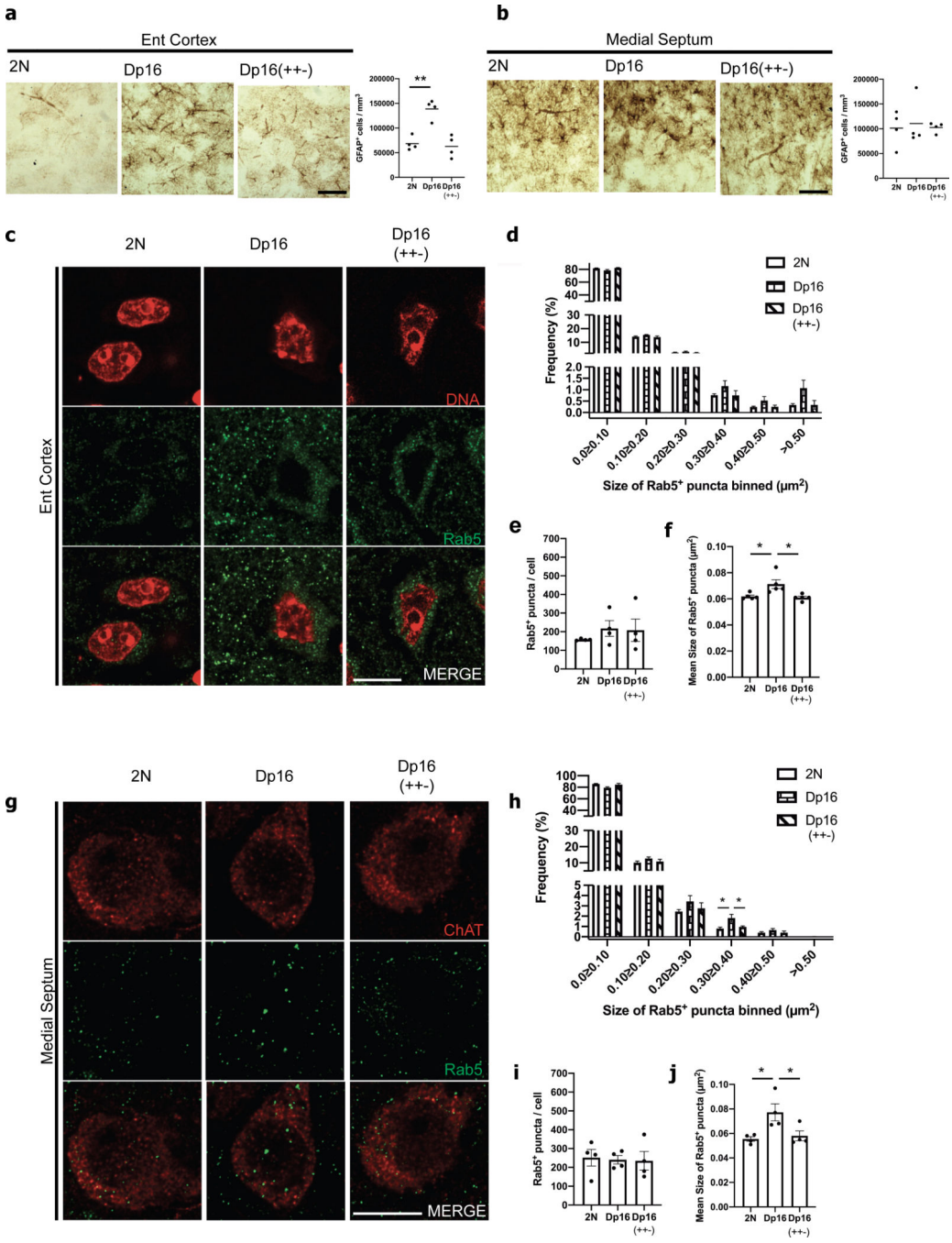

Figure 5. AD-relevant phenotypes in astrocytes and endosomes in the entorhinal cortex and medial septum in Dp16, Dp16(m*App* ++-), and 2N mice.

Dp16, Dp16(m*App*++-), and 2N mice were evaluated at age 4 months. Photomicrographs of GFAP immunoreactivity and quantification of the number of positive astrocytes per mm^3 in the (a) entorhinal cortex and (b) medial septum. Measurements were from 4-fields per animal with 4 animals per group. (c) Representative images from the entorhinal cortex of Rab5-positive punctae (green) surrounding the nuclei (red). (d) quantitative analysis of the binned size distribution of Rab5-positive punctae; (e) the number of rab5-positive punctae per cell; and (f) the mean area of rab5-positive punctae (2N: 0.06 μm^2; Dp16(m*App*++-):

0.06 μm^2; Dp16: 0.07 μm^2). (g) Representative images from medial septum BFCN of Rab5-positive punctae (green) within choline acetyltransferase positive cells (red). (h) Quantitative analysis of the binned size distribution of Rab5-positive punctae; (i) the number of rab5-positive punctae per cell; and (j) the mean area of rab5-positive punctae (2N: 0.06μm^2; Dp16(m*App*++-): 0.06 μm^2; Dp16: 0.08 μm^2). Scale bar in a and b = 100 μm; c and g = 10 μm. Statistical analysis: N=4; all values are means with error bars indicating the S.E.M, and p values were calculated using a one-way ANOVA and Dunnett's multiple comparisons test; (* = p<.05, and ** = p<0.01).

Alzheimers Dement. Author manuscript; available in PMC 2023 June 01.

Table 1.

Demographics of the human postmortem specimens.

Origin	Category	Case#	Sex	Age	PMI	Clinical Diagnosis	Additional Comments	Braak Stage	Amyloid Plaque Status	*APOE* eX/eX status (where X = 2, 3, and/or 4)	WB	Aβ
SHRI	**ND**	10–70	M	74	3.25	Cognitively normal	Pancreatic cancer	I	0 [a]	2/3	x	x
SHRI	**ND**	12–70	M	74	4.58	Cognitively normal	Lung cancer	III	1 [a]	NA	x	x
SHRI	**ND**	10–63	M	79	3	Cognitively normal		II	0 [a]	3/3	x	x
SHRI	**ND**	09–57	M	80	3.5	Cognitively normal	Pancreatic cancer	III	1 [a]	2/2	x	x
UCI	**ND**	9–03	M	81	6.4	Normal		II	0 [b]	2/3	x	x
UCI	**ND**	25–01	M	83	1.8	Normal		II	0 [b]	3/3	x	x
UCI	**ND**	12–16	M	83	3.18	Normal		II	0 [b]	3/3		x
ADRC	**ND**	X5783	M	84	36	Normal for age		II	0 [c]	2/3	x	x
ADRC	**ND**	X5687	M	84	8	Normal	Acute ischemic changes	I	0 [c]	3/3	x	x
UCI	**ND**	11–12	M	86	4.42	Normal		II	0 [b]	3/3	x	x
SHRI	**ND**	10–39	M	93	3	Cognitively normal		I	0 [a]	3/3	x	x
ADRC	**ND**	X5709	M	94	12	Normal		II	0 [c]	3/3	x	x
UCI	**AD-DS**	13–02	M	46	6.37	Trisomy 21 (dementia)		VI	Stage C [b]	NA	x	x
UCI	**AD-DS**	31–08	M	49	2.2	Trisomy 21 (dementia)		VI	Stage C [b]	NA	x	x
UCI	**AD-DS**	42–08	M	55	4.5	Trisomy 21 (dementia)		VI	Stage C [b]	NA	x	x
UCI	**AD-DS**	4–16	M	70	3.92	Trisomy 21 (dementia)		VI	Stage B [b]	3/3	x	x
UCI	**PT-DS**	27–15	M	72	4.87	Partial Trisomy 21	Cognitively normal [28]	III	0 [b]	2/3	x	x
SHRI	**AD**	11–38	M	64	2.33	AD		VI	3 [a]	3/3	x	x
SHRI	**AD**	13–10	M	74	2.58	Probable AD		VI	3 [a]	3/4	x	x
UCI	**AD**	1–01	M	81	2.5	AD		VI	Stage C [b]	3/4	x	x

Origin	Category	Case#	Sex	Age	PMI	Clinical Diagnosis	Additional Comments	Braak Stage	Amyloid Plaque Status	*APOE* εX/εX status (where X = 2, 3, and/or 4)	WB	Aβ
SHRI	**AD**	11–78	M	82	2.95	Mixed vascular dementia		V	3 [a]	3/3		x
UCI	**AD**	4–02	M	83	3.4	AD		VI	Stage C [b]	NA		x
ADRC	**AD**	X5812	M	84	16	AD, Other	Severe, Diffuse Lewy Body Disease, amygdala predominant type. Old infarcts - left temporal lobe, left posterior inferior cerebellar hemisphere.	VI	4 [c]	3/4	x	x
ADRC	**AD**	X5770	M	84	6	AD	Severe, Diffuse Lewy body disease, limbic (transitional) type.	VI	5 [c]	3/3	x	x
UCI	**AD**	32–18	M	85	5.75	AD	Severe, Diffuse Lewy body disease	VI	Stage B [b]	3/4	x	x
UCI	**AD**	1–02	M	88	3	AD	Severe, Diffuse Lewy body disease	VI	Stage C [b]	3/4	x	x
SHRI	**AD**	11–27	M	89	2.2	Probable AD	Severe, Diffuse Lewy body disease	V	3 [a]	2/3	x	x
Origin	**Category**	**Case#**	**Sex**	**Age**	**PMI**	**Diagnosis**	**Additional Comments**	**Braak Stage**	**Amyloid Plaque Status**	**ApoE**	**WB**	**Aβ**
SHRI	**ND**	11–98	F	58	3.13	Cognitively normal		I	0 [a]	2/3	x	x
SHRI	**ND**	10–22	F	59	3.13	Cognitively normal	Metastatic adrenocortical carcinoma, stage IV	I	0 [a]	3/3	x	x
ADRC	**ND**	X5628	F	80	12	Normal		I	0 [c]	3/3	x	x
ADRC	**ND**	X5302	F	83	72	Normal		I	1 [c]	2/4		x
UCI	**ND**	19–13	F	87	3.83	Normal		III	0 [b]	2/3		x
ADRC	**ND**	X5248	F	93	18	Normal		I	0 [c]	3/3	x	x
SHRI	**ND**	10–26	F	95	2.5	Cognitively normal		III	0 [a]	3/3	x	x
ADRC	**ND**	X5049	F	102	9	Normal		I	0 [c]	3/3	x	x
UCI	**AD-DS**	29–06	F	45	2.75	Trisomy 21 (dementia)		VI	Stage C [b]	3/3	x	x
UCI	**AD-DS**	1–11	F	45	2.7	Trisomy 21 (dementia)	Vascular Dementia (Amyloid Angiopathy)	VI	Stage C [b]	3/3	x	x
UCI	**AD-DS**	7–17	F	47	6.5	Trisomy 21 (dementia)		VI	Stage C [b]	NA	x	x

Origin	Category	Case#	Sex	Age	PMI	Clinical Diagnosis	Additional Comments	Braak Stage	Amyloid Plaque Status	*APOE* εX/εX status (where X = 2, 3, and/or 4)	WB	Aβ
UCI	**AD-DS**	33–04	F	50	5	Trisomy 21 (dementia)		VI	Stage C [b]	3/4	x	x
UCI	**AD-DS**	31–07	F	52	4.37	Trisomy 21 (dementia)		VI	Stage C [b]	NA	x	x
UCI	**AD-DS**	08–08	F	57	5.28	Trisomy 21 (dementia)		VI	Stage C [b]	NA	x	x
UCI	**AD-DS**	31–10	F	62	2.42	Trisomy 21 (dementia)		VI	Stage C [b]	3/3	x	x
UCI	**DS**	32–08	F	42	5	Trisomy 21 (no dementia)		V	Stage C [b]	3/4	x	x
UCI	**DS**	35–06	F	48	18.35	Trisomy 21 (no dementia)	mosaic	III	Stage B [b]	3/3	x	x
UCI	**DS**	5–15	F	51	2.72	Trisomy 21 (no dementia)		III	Stage C [b]	2/3	x	x
UCI	**DS**	33–17	F	62	7.03	Trisomy 21 (no dementia)		III	Stage B [b]	NA	x	x
ADRC	**AD**	X5692	F	80	1	AD	Diffuse Lewy body disease, Hemorrhage	V	5 [c]	3/3	x	x
ADRC	**AD**	X5799	F	82	15	AD	Severe	VI	5 [c]	4/4		x
UCI	**AD**	27–00	F	83	2.4	AD		NA	Stage C [b]	3/3		x
SHRI	**AD**	11–46	F	84	2.53	DLB		V	3 [a]	3/3		x
UCI	**AD**	37–15	F	87	4.25	AD		VI	Stage C [b]	3/4		x
ADRC	**AD**	X5798	F	87	7	AD	Diffuse Lewy body disease	V	5 [c]	3/3	x	x
SHRI	**AD**	12–27	F	89	2.7	Probable AD		VI	3 [a]	2/3	x	x
UCI	**AD**	15–05	F	89	3.4	AD		VI	Stage C [b]	3/4	x	x
SHRI	**AD**	11–35	F	93	2.83	Probable AD		VI	3 [a]	3/3	x	x
ADRC	**AD**	X5792	F	93	10	AD	Infarct, Alzheimer type II astrocytes, consistent with terminal metabolic encephalopathy	V	4 [c]	3/3	x	x
ADRC	**AD**	X5583	F	94	14	AD		IV	4 [c]	3/3	x	

Specimens and their diagnoses were provided by the following brain banks: SHRI = Banner Sun Health Research Institute; UCI = UCI-ADRC Brain tissue repository; ADRC = UCSD-ADRC. PMI = postmortem interval in hours. There were no significant differences between groups for PMI when evaluating the full data set. Outlier analysis was then performed using GraphPad Prism 8. ROUT outlier analysis identified 5 cases X5783 (ND, 36 hrs); ND:X5302 (ND, 72 hrs); X5812 (AD, 16 hrs); X5799 (AD, 15 hrs); X5583 (AD, 14 hrs). One-way ANOVA analysis of PMI indicated no significant

Alzheimers Dement. Author manuscript; available in PMC 2023 June 01.

differences between groups when outliers were removed. Tau pathology from all tissue sources was based on Braak and Braak (1991) [56]. For SHRI cases plaque score was based on CERAD (Consortium to Establish a Registry for Alzheimer's disease, highlighted in yellow) score [54]. CERAD templates were used to obtain semi-quantitative scores of neuritic and/or cored plaque density and cases were scored as none (0), sparse (1), moderate (2), and frequent (3). The value listed represents the highest density score seen in any of the three evaluated cerebral neocortex regions (frontal, temporal, and parietal). For ADRC cases Aβ-deposition was scored based on the Thal phase (highlighted in purple) [55]. For UCI cases plaque pathology is based on Braak and Braak [56]. APOE genotype is listed where known. NA = not available. Cases analyzed with western blots are marked with an "x" and highlighted in orange and those with MSD in green. The identification of the samples on the western blots shown in the Figures will be provided upon request.

[a]CERAD neuritic plaque frequency at maximum density in neocortex (0, sparse, moderate, frequent or 0–3) [54].

[b]Amyloid plaque stages – 0, A, B, and C [56].

[c]Thal amyloid phase (0–5) [55]. ND: non-demented controls; PMI: postmortem interval; WB: submitted to western blot analysis; Aβ: submitted to analysis for Aβ levels.

Table 2.

Transcriptional alterations of AD-related genes.

Analysis using the NanoString AD panel. Genes showing significant differences ($p < 0.05$) and changes more than ± 25% between 2N and Dp16 mice are shown at 4 months (upper panel) and 19 months (lower panel). Down-regulated genes compared to 2N are highlighted in blue, genes up-regulated more than 50% in red, and up-regulated between 25 and 50% in orange. n = 3 for all samples. Accession number, Chromosome number (Chr#), and official full name are listed.

Gene Name	Ratio	P-value	Accession	Chr #	Official Full Name
Plekha7	**0.54**	0.0204	NM_172743.2	7	pleckstrin homology domain containing, family A member 7
Olfm3	**0.54**	0.0473	NM_153157.3	3	olfactomedin 3
Per1	**0.64**	0.0089	NM_011065.4	11	period circadian clock 1
Rell1	**0.68**	0.0336	NM_145923.2	5	RELT-like 1
Ano6	**1.32**	0.0401	NM_175344.4	15	anoctamin 6
Ctss	**1.46**	0.0052	NM_021281.2	3	cathepsin S
App	**1.46**	0.006	NM_007471.2	**16**	amyloid beta (A4) precursor protein
Synj1	**1.46**	0.0254	NM_001045515.1	**16**	synaptojanin 1
Psmg1	**1.51**	0.007	NM_019537.2	**16**	proteasome (prosome, macropain) assembly chaperone 1

Dp16 vs 2N mice at 19 months of age					
Gene Name	**Ratio**	**P-value**	**Accession**	**Chr #**	**Official Full Name**
Aph1a	**1.28**	0.0206	NM_146104.2	3	aph1 homolog A, gamma secretase subunit
Golim4	**1.29**	0.0196	NM_001291069.1	3	Golgi integral membrane protein 4
Tbc1d9	**1.31**	0.0385	NM_001111304.1	8	TBC1 domain family, member 9
Samd4	**1.33**	0.0104	NM_028966.3	14	sterile alpha motif domain containing 4
Man2a1	**1.35**	0.0107	NM_008549.2	17	mannosidase 2, alpha 1
Psmg1	**1.38**	0.0057	NM_019537.2	**16**	proteasome (prosome, macropain) assembly chaperone 1
Synj1	**1.41**	0.0006	NM_001045515.1	**16**	synaptojanin 1
App	**1.49**	0.0002	NM_007471.2	**16**	amyloid beta (A4) precursor protein
Fxyd5	**1.55**	0.0301	NM_008761.3	7	FXYD domain-containing ion transport regulator 5

Table 3.

Summary of Findings and Comparison Between AD-DS and the Dp16 Mouse

Parameter	AD-DS Male	AD-DS Female	Dp16 Mouse	Dp16 Mouse Similar to AD-DS?	Notes/ References
fl-APP; *vs APP* gene copy number	increased; not beyond copy number	increased; not beyond copy number	increased; not beyond copy number	yes; yes	[34, 37, 38]
CTFs; vs fl-APP	increased; not beyond fl-hAPP	increased; greater than fl-hAPP (**)	increased; beyond fl-mApp at 19 mos in male hippo	yes; yes	(**) sex effect in AD-DS in this study; [37, 39]; untested whether aged Dp16 males and females differ.
Aβ42; vs fl-APP; increased with age	increased; beyond fl-hAPP; yes	increased; beyond fl-hAPP; yes	increased; not beyond fl-mApp; yes	yes; no; yes	[34, 37, 164–167]
Aβ40; vs fl-hAPP; increased with age	increased; beyond fl-hAPP; yes	increased; beyond fl-hAPP; yes	increased; not beyond fl-mApp; yes	yes; no; yes	[34, 37, 165–167]
Aβ38; vs fl-APP	increased; beyond fl-hAPP	increased; not beyond fl-hAPP	[a]ND	[b]NA	
Aβ-containing amyloid plaque pathology; *APP* copy number dependent	yes; yes	yes; yes	NA	NA	[20, 21, 27, 28, 36, 40, 168]; We are not aware of reports of significant amyloid plaque pathology in mice expressing wild-type mouse *APP.*
Levels of APP processing enzymes vs ND or 2N	no significant changes	increased BACE2, Nicastrin (mature), BACE1 (mature), and PEN2 (**)	trend to increased BACE 1 in female vs 2N and female versus male (##)	yes	(**) sex effect in AD-DS in this study; (##) possible sex effect in Dp16 in this study: no change in BACE 1 or 2 protein levels in a DS series containing both males (n = 18) and females (n = 10) whose ages (34.3 ± 21.2 years) put them at increased risk for AD-DS [34].
Decreased neuron number; *APP* copy number dependent	yes: [c]TBD	yes; TBD	yes; yes	yes; TBD	[87, 89, 91, 93]
Increased pT212; increased total tau (versus ND or 2N)	yes; yes	yes; yes	yes for pT212; no increase total tau	yes; no	pT212 [169]; increased tau mRNA [33]; increased tau protein [170, 171] in DS cases > 40 years of age
Increased tau pathology versus ND or 2N; neurofibrillary tangles; *APP* copy number dependent	yes; yes; yes	yes; yes; yes	yes; no; yes	yes; NA; yes	[19, 27, 28, 101, 168, 172–174] in DS cases > 40 years of age. We are not aware of reports of neurofibrillary tangles in mice expressing wild-type tau.
Endosomal abnormalities versus ND or 2N; APP copy number dependent	TBD; TBD	TBD; TBD	yes; yes	TBD; TBD	Evidence from young DS indicate abnormalities [24] from a very early age. While this is likely to be the case in AD-DS, we are not aware of reports of abnormal endosomes in AD-DS.
Microglial abnormalities versus ND or 2N; *APP* copy number dependent	yes; TBD	yes; TBD	yes; yes	yes; TBD	[22, 25, 175]

[a]ND = not determined

[b]NA = not applicable

[c] TBD = to be determined